Published in final edited form as:
Am J Obstet Gynecol. 2011 January ; 204(1): 84.e1–84.e27. doi:10.1016/j.ajog.2010.08.043.

A transcriptional profile of the decidua in preeclampsia

Mari LØSET[*], **Siv B. MUNDAL**[*], **Dr. Matthew P. JOHNSON, PhD**, **Dr. Mona H. FENSTAD, MD**, **Dr. Katherine A. FREED, PhD**, **Dr. Ingrid A. LIAN, MD**, **Dr. Irina P. EIDE, MD, PhD**, **Dr. Line BJØRGE, MD, PhD**, **Dr. John BLANGERO, PhD**, **Dr. Eric K. MOSES, PhD**, and **Dr. Rigmor AUSTGULEN, MD, PhD**

Department of Cancer Research and Molecular Medicine (Løset, Mundal, Drs Fenstad, Lian and Austgulen), Faculty of Medicine, Norwegian University of Science and Technology (NTNU), Trondheim, Norway; Central Norway Regional Health Authority (Dr Eide), Trondheim, Norway; Department of Genetics (Drs Johnson, Freed, Blangero and Moses), Southwest Foundation for Biomedical Research, San Antonio, Texas, USA; Department of Obstetrics and Gynecology (Dr Bjørge), Haukeland University Hospital, Bergen, Norway

Abstract

OBJECTIVE—To obtain insight into possible mechanisms underlying preeclampsia using genome-wide transcriptional profiling in decidua basalis.

STUDY DESIGN—Genome-wide transcriptional profiling was performed on decidua basalis tissue from preeclamptic (n = 37) and normal pregnancies (n = 58). Differentially expressed genes were identified and merged into canonical pathways and networks.

RESULTS—Of the 26,504 expressed transcripts detected, 455 were differentially expressed (*P* <0.05, FDR *P* <0.1). Both novel (ARL5B, SLITRK4) and previously reported preeclampsia-associated genes (PLA2G7, HMOX1) were identified. Pathway analysis revealed that ‘tryptophan metabolism’, ‘endoplasmic reticulum stress’, ‘linoleic acid metabolism’, ‘notch signaling’, ‘fatty acid metabolism’, ‘arachidonic acid metabolism’ and ‘NRF2-mediated oxidative stress response’ were overrepresented canonical pathways.

CONCLUSION—In the present study single genes, canonical pathways and gene-gene networks that are likely to play an important role in the pathogenesis of preeclampsia, have been identified. Future functional studies are needed to accomplish a greater understanding of the mechanisms involved.

Keywords

decidua; genome-wide gene expression; microarray; preeclampsia

Corresponding author: MD/PhD student Mari Løset, Department of Cancer Research and Molecular Medicine, Norwegian University of Science and Technology, Olav Kyrres gate 11, N-7006 Trondheim, Norway. Tel.: +47 90 79 91 17, fax: +47 72 57 47 04. maril@stud.ntnu.no.
[*]Authors have contributed equally to this work.

Reprints: MD/PhD student Mari Løset, Department of Cancer Research and Molecular Medicine, Norwegian University of Science and Technology, Olav Kyrres gate 11, N-7006 Trondheim, Norway. maril@stud.ntnu.no

INTRODUCTION

The etiology of preeclampsia is not fully understood, but a number of observations suggest that divergent abnormalities may be involved (immunological, inflammatory, vascular/ischemic).[1] In a normal pregnancy extravillous trophoblasts (of fetal origin) invade decidua basalis and modify the spiral arteries. In preeclampsia, this pregnancy-associated adaption of spiral arteries may fail, with a hypoperfused placenta as a result. Oxidative stress is suggested to play a central role in the pathogenesis of preeclampsia,[2] and may be generated in the decidua basalis.[3, 4] Heritability of the disease has been estimated to be greater than 50%,[5, 6] with both maternal and fetal (paternal) contributions.[7]

Microarray-based transcriptional profiling can be a powerful strategy for identification of disease-related genes and pathways,[8] and this approach has been used for analysis of placental[9] as well as decidual tissues[6, 10, 11] from preeclamptic pregnancies. However, the data obtained have been inconsistent. In the case of the three decidual studies reported, the diverging results may be due to the relatively small number of samples analysed (≤12 preeclamptic samples included).[6, 10, 11] In the current study we have applied genome-wide transcriptional profiling (measuring ≥48,000 transcripts from all known genes) on a large collection of decidual samples (from 37 preeclamptic and 58 normal pregnancies) to comprehensively investigate how gene expression at the maternal-fetal interface may be contributing to the pathogenesis of preeclampsia. We further aimed to identify the genetic canonical pathways and gene-gene interaction networks represented by the differently expressed genes using contemporary bioinformatic approaches.

MATERIALS AND METHODS

Human subjects

Women with pregnancies complicated by preeclampsia (n = 43) and women with normal pregnancies (n = 59) were recruited at St. Olavs' University Hospital (Trondheim, Norway) and Haukeland University Hospital (Bergen, Norway) from 2002 to 2006. Preeclampsia was defined as persistent hypertension (blood pressure of ≥140/90 mmHg) plus proteinuria (≥0.3 g/L or ≥1+ by dipstick), developing after 20 weeks of pregnancy.[12] Due to tissue sampling procedures, only pregnancies delivered by caesarean section were included. Women with preeclamptic pregnancies had caesarean section performed for medical indications, whereas women with normal pregnancies underwent caesarean section for reasons considered irrelevant to the aim of the study (e.g. breech presentation, cephalopelvic disproportion in previous delivery and fear of vaginal delivery). None of the included mothers were in labour prior to caesarean section. Exclusively healthy women with no history of preeclampsia were accepted in the normal pregnancy group. Multiple pregnancies, pregnancies with chromosomal aberrations, fetal and placental structural abnormalities or suspected perinatal infections were excluded from both study groups. The study was approved by the Norwegian Regional Committee for Medical Research Ethics. Informed consent was obtained from all participants prior to collection of decidual samples.

Decidual tissue collection

Samples of decidua basalis tissue were obtained by vacuum suction of the placental bed, a procedure which allows the collection of tissue from the whole placental bed.[13] Collected samples were flushed with saline solution to remove excessive blood. The decidual tissue was immediately submerged in RNA-later (Ambion, Huntington, UK) and stored at −80°C.

Total RNA isolation

Total RNA was isolated using a trizol extraction protocol with chloroform interphase separation, isopropanol precipitation and ethanol wash steps. Precipitated total RNA was re-suspended in RNase free water and purified with an RNeasy Mini Kit using spin technology (Qiagen, Valencia, CA). Spectrophotometric determination of purified total RNA yield (μg) was performed using the NanoDrop ND-1000 (Wilmington, DE). Total RNA quality was measured using Agilent's RNA 6000 Nano Series II Kit on a BioAnalyzer 2100 (Agilent Technologies, Germany). Ethical approval for total RNA processing and decidua expression analysis was obtained from the Institutional Review Board at The University of Texas Health Science Center in San Antonio.

Synthesis, amplification and purification of anti-sense RNA

Anti-sense RNA (aRNA) was synthesized, amplified and purified using the Illumina TotalPrep RNA Amplification Kit according to manufacturers' instructions (Ambion, Austin TX). Synthesis of aRNA was performed using a T7 Oligo(dT) primer and the amplification underwent *in vitro* transcription with a T7 RNA polymerase to generate multiple copies of biotinylated aRNA from a double-stranded cDNA template. Purified aRNA yield was determined spectrophotometrically using the NanoDrop ND-1000.

Microarray data

Purified aRNA was hybridized to Illumina's HumanWG-6 v2 Expression BeadChip (Illumina Inc. San Diego, CA). Washing, blocking and transcript signal detection (streptavidin-Cy3) was performed using Illumina's 6×2 BeadChip protocol. Samples were scanned on the Illumina BeadArray 500GX Reader using Illumina BeadScan image data acquisition software (version 2.3.0.13). Illumina's BeadStudio Gene Expression software module (version 3.2.7) was used to subtract background noise signals and generate an output file for statistical analysis.

Real-time RT-qPCR

We performed a technical replicate of the microarray experiment with quantitative real-time RT-PCR on six of the most differentially expressed transcripts using a 7900HT Fast Real-Time PCR instrument (Applied Biosystems, Foster City, CA). The six genes were prioritized for real-time RT-PCR based on beta values, FDR *P*-values and manual literature searches. Real-time RT-qPCR was run with 93 samples. Two of the total collection of 95 samples were excluded due to shortage of biological material. Pre-optimized TaqMan Gene Expression Assays (Applied Biosystems) were run, in triplicate, to measure mRNA expression levels relative to the reference genes, TBP and GAPDH. Reverse transcription and PCR amplification was performed in a two-step procedure, following Applied Biosystems High-Capacity cDNA ReverseTranscription Kit Protocol and TaqMan Gene Expression Master Mix Protocol. Negative controls were run, in triplicate, without RT enzyme or no cDNA template.

Statistical analysis

Transcript data for each sample was pre-processed and analysed using SOLAR[14] as previously described.[15] To evaluate the magnitude of differential gene expression the displacement of each detected transcript's mean expression value was measured between the two groups. A standard regression analysis was performed on the preeclamptic group to test whether the mean transcription level differed from that of the normal pregnancy group.

The mRNA expression levels were calculated by the Comparative CT method as described elsewhere.[16] For each target gene, the mean CT value for each sample was used for analysis,

after exclusion of outliers. Outliers were determined as values more than 2SD from the mean. Delta CT (ΔCT) values were computed as the difference between the given mean value for a target gene and the mean of the CT values for the two reference genes.[17] Fold change values were calculated, based on the differences in ΔCT values between tissue from preeclamptic women and normal pregnant women ($2^{-\Delta\Delta CT}$).[16] A t-test statistic (SPSS 16.0) evaluated the difference between the ΔCT values of the preeclamptic pregnancies, as compared to the normal pregnancy group. Analysing for the two reference-genes separately did not change the results.

Canonical pathway and network identification

Differentially expressed transcripts in the preeclamptic group (P <0.05, false discovery rate (FDR)[18] P <0.1) were imported into Ingenuity Pathways Analysis (IPA) v7.5 (www.ingenuity.com). Transcripts' gene identifiers were mapped to their corresponding gene object in the Ingenuity Pathways Knowledge Base. IPA was used to bioinformatically identify canonical (i.e. cell signalling and metabolic) pathways and gene-gene interaction networks potentially involved in preeclampsia within our data set. IPA gene-gene networks were constructed from the published literature and they diagrammatically represent molecular relationships between gene-gene products.

Significant IPA pathways were further analyzed with Rotation Gene Set Enrichment Analysis (ROMER) pathway analysis, using the *limma* package, available via the Bioconductor Project (www.r-project.org).[19]

RESULTS

Human Subjects

The clinical information of women/pregnancies enrolled is presented in Table 1. Only those samples of sufficient RNA quality for gene expression analysis have been included. In the preeclamptic pregnancies, both mean gestational age and birth weight were lower than in the normal pregnancies (Table 1). As expected, the mean blood pressure was higher among preeclamptic than normal pregnancies (Table 1).

Decidual genome-wide transcriptional profiling

In total, 43 women with pregnancies complicated by preeclampsia and 59 women with normal pregnancies were included in the study. Six samples from preeclamptic pregnancies and one sample from a normal pregnancy were excluded from gene expression analyses due to low RNA quality. The 95 samples with good RNA quality were hybridized onto Illumina's HumanWG-6 v2 genome-wide expression beadchip.

The non-normalized decidua basalis transcriptional profile data (n = 48,095) may be found at ArrayExpress (http://www.ebi.ac.uk/microarray-as/ae/) (accession code E-TABM-682). We detected 26,504 significantly expressed transcripts (55.1%), of which 455 were differentially expressed after FDR correction (P <0.05, FDR P <0.1); 285 were down-regulated and 170 were up-regulated. The significant differentially expressed transcripts are presented in Table 2 together with the corresponding P values (raw and FDR adjusted) and preeclampsia-correlated expression. The real-time RT-qPCR for the six genes (PLA2G7, ANGPTL2, MAN1A2, SLITRK4, FZD4 and ARL5B) tested showed a high grade of correlation with the microarray data (Table 3).

Canonical pathways and network

The 455 differentially expressed transcripts were analyzed using IPA. The significant canonical pathways (P <0.01) are shown in Table 4, along with the included genes and P

values. They included ‘tryptophan metabolism’, ‘endoplasmic reticulum stress’, ‘linoleic acid metabolism’, ‘notch signaling’, ‘fatty acid metabolism’, ‘arachidonic acid metabolism’ and ‘NRF2-mediated oxidative stress response’. All the canonical pathways identified in IPA were also found to be significant (P <0.01) using ROMER (Table 4), with the exception of the ‘NRF2-mediated oxidative stress response’ canonical pathway (IPA P = 0.009, ROMER P = 0.067).

Using network analysis in IPA, 59 of the preeclampsia associated genes could be connected into a single network of gene-gene product interactions (Figure 1). The genes in this network were among others involved in the function of endoplasmic reticulum (ER), oxidative stress, notch signaling and cell migration. The network included a cluster of 15 up-regulated genes (ATP2A2, TRAM1, FKBP2, HMOX1, SPCS2, ATF6, DNAJC3, EIF2AK3, PIGA, SEC23B, SEC24D, DNAJB9, SRPRB, DNAJB11 and XBP1) associated with ER stress and oxidative stress (Figure 1). All these genes were in a direct relationship to X-box binding protein 1 (XBP1). Epidermal growth factor receptor (EGFR) was another focus molecule with a direct relationship to seven other genes (PLCG1, NGF, MET, LRIG1, SLN, ATP2A2 and SHC2) in the network.

COMMENT

In this study, 455 differentially expressed transcripts were found when decidua basalis tissue from preeclamptic and normal pregnancies was compared. Some transcripts were novel findings (i.e., ARL5B and SLITRK4), whereas others, such as PLA2G7[20] and HMOX1[21, 22] have been reported to be associated to preeclampsia previously. Pathway analysis identified seven significant canonical pathways.

In our patient cohort, a lower gestational age was found in the preeclamptic group (average 32 weeks: range 28–36) as compared to the normal pregnancy group (39 weeks: range 38–40). This is not unexpected due to the need for early delivery in patients with severe preeclampsia. Since gene expression in uteroplacental tissues may be influenced by gestational age,[23, 24] it cannot be excluded that some of the differences observed between the preeclamptic and normal pregnancy groups are in fact gestational age related. Winn et al compared global gene expression in basal plate (decidual) biopsies from normal pregnancies at mid-gestation (14 – 24 wk) and at term (37 – 40wk)[23] and found that 418 genes (of 39,000 transcripts examined) changed expression throughout gestation. This provides a useful dataset for comparison with the data obtained in this current study, albeit different profiling platforms were used. Winn et al used the Affymetrix HG-U133 A&B chip for transcriptional profiling whereas we used the Illumina HumanWG-6 v2 Expression BeadChip. By this, the number of possible comparisons was restricted to the 16,799 genes shared in both systems. Of the 455 transcripts found to be differentially expressed in this current study, 368 genes demonstrate no gestational age influenced changes, according to the data of Winn et al.[23] It is therefore tempting to speculate that the differential expression of these 368 genes may be related to disease mechanisms at play in preeclampsia. Seventeen of our differentially expressed genes (TEMEM97, KIAA1598, SULT2B1, EGFR, FHL1, PLA2G7, SHANK3, NOTCH4, UBASH3B, ROBO4, NRARP, GPR116, IL6ST, LDLR, ANGPTL2, SRPRB, KREMEN1) are reported to change expression with gestational age.[23] For two of these genes (SULT2B1, EGFR), expression increases towards term.[23] Thus, isolated gestational age related influences in the preeclampsia group would suggest a lower expression of SULT2B1and EGFR, but both were up-regulated in our dataset. Similarly, the ANGPTL2 gene is down-regulated towards term,[23] but in contrast to what might be expected from gestational age related changes, expression was lower in the preeclampsia group than in the normal pregnancy group. Based on this, we conclude that the differential expression of these three genes may also be ascribed to disease related mechanisms.

However, with regard to the remaining 14 genes in our dataset previously shown to exhibit gestational age dependent changes in expression, conclusions are hampered by the fact that gestational age may have contributed to the differences observed between preeclamptic and normal pregnancies. To illustrate; expression of FHL1, SHANK3, NOTCH4, ROBO4, NRARP and GPR116 increase towards term[23] and were down-regulated in the preeclampsia group, whereas TMEM97, KIAA1598, PLA2G7, UBASH3B, IL6ST, LDLR, SRPRB and KREMEN1 expression decrease towards term[23] and were up-regulated in the preeclampsia group.

In genome-wide transcriptional profiling, analysis of *groups* of genes is a strategy to increase power and reduce the dimensionality of the underlying statistical problem following multiple testing.[25] Further, it may be advantageous to put focus on canonical pathways and networks instead of single genes when the aim is to obtain insight in the pathophysiology of complex diseases, such as preeclampsia. The high interconnectivity of focus genes with other correlated genes within a biological network may imply functional and biological importance of these genes.[26, 27] To be able to assess this in a comprehensive manner, we increased the FDR cut off to 0.1 and consequently the number of genes included in the analysis. Using this approach, seven significant canonical pathways were found to be represented by the differentially expressed genes identified in this current study (Table 4).

The most significant canonical pathway detected was ‘tryptophan metabolism’. The metabolism of tryptophan, through the kynurenine pathway, has previously been suggested to be involved in preeclampsia pathogenesis,[28, 29] and in accordance with this, the activity of the first enzyme of the kynurenine pathway, indoleamine 2,3 dioxygenase (IDO), has been reported to be reduced in placenta from preeclamptic pregnancies.[28] We found no disease-associated changes in IDO expression, but the transcript encoding the enzyme kynureninase (KYNU) was up-regulated. KYNU metabolises L-kynurenine, which suppresses T-cell proliferation and natural killer cells and influences immunotolerance to foreign antigens.[30] This implies that a consequence of KYNU up-regulation may be an increased inflammatory response (due to lack of L-kynurenine). An additional seven genes were assigned to this canonical pathway (Table 4).

The second most significant canonical pathway identified was the ‘endoplasmic reticulum stress pathway’. Three genes (EIF2AK3, ATF6 and XBP1) included in the unfolded protein response (UPR), a coordinated adaptive response to ER stress, were up-regulated. ER stress has previously been suggested as one of the main sources for generation of placental oxidative stress.[31] Yung et al have reported similar associations of the UPR signalling pathways to preeclampsia in placental tissue[32] but these findings are reported for the first time in decidual tissue. There is a close connection between oxidative stress and ER stress, [31, 33] also indicated by the many direct relationships of the ER and oxidative stress related genes in the generated network (Figure 1). The canonical pathway ‘NRF2-mediated oxidative stress response’ was also among the significant pathways identified (Table 4). The nuclear factor NFR2 plays an essential role in the defence of oxidative stress by regulating the expression of antioxidant response elements (AREs).[34] In case of excessive oxidative stress, activation by ROS, NO and pro-inflammatory cytokines, result in translocation of NRF2 to the nucleus. NRF2 binds to ARE sequences, leading to transcriptional activation of antioxidant genes (e.g. glutathione and HMOX1). ‘NRF2-mediated oxidative stress response’ included nine genes, of which three genes have previously been associated with preeclampsia; EIF2AK3,[32] GSTA3[10] and HMOX1.[21, 22] Several enzymes metabolize ROS to exportable compounds, and in this study the transcripts encoding the antioxidant enzymes GSTA3, HMOX1 and UBE2K were up-regulated.

Three of the remaining significant canonical pathways generated by IPA represented metabolism of fatty acids; 'linoleic acid metabolism', 'fatty acid metabolism' and 'arachidonic acid metabolism'. The genes included in these pathways were partly overlapping, as shown in Table 4. Decidual arterioles of preeclamptic women show atherosclerotic-like lesions,[35] suggesting an underlying atherogenic process of LDL lipid peroxidation.[36] Lipid peroxidation contributes to the development of preeclampsia,[37] and decidua basalis tissue from preeclamptic women has an increased content of lipid peroxides.[4] The first enzyme of the fatty acid β-oxidation pathway, acyl-coenzyme A oxidase 1 (ACOX1)/palmitoyl-coA oxidase, donates electrons directly to molecular oxygen, thereby producing hydrogen peroxides. ACOX1 was found to be up-regulated, whereas acyl-coenzyme A oxidase 2 (ACOX2)/branched chain acyl-coA oxidase, which is involved in the degradation of long branched fatty acids and bile acid intermediates in peroxisomes, was found to be down-regulated. Two genes involved in elimination of lipid peroxidation products were also down-regulated in the material, alcohol dehydrogenase 1a (ADH1A), which metabolizes a wide variety of substrates including lipid peroxidation products, and aldehydedehydrogenase 3 family member A2 (ALDH3A2) isozymes, thought to play a major role in the detoxification of aldehydes generated by alcohol metabolism and lipid peroxidation. Increased generation or decreased elimination of lipid peroxidation products may be among the factors activating the maternal endothelium[38] and triggering systemic inflammation in preeclampsia.

Finally, the pathway analysis suggested a role of 'notch signalling', with inclusion of four down-regulated genes; DTX3, HES1, NOTCH 3 and NOTCH 4. Notch signalling is known to be involved in cell differentiation, proliferation, apoptosis[39] and blood vessel formation,[40] processes neatly regulated in the placenta to maintain a normal pregnancy. Notch receptors are expressed on extravillous trophoblasts and are hypothesised to be involved in the differentiation and proliferation of both extravillous trophoblasts and endothelial cells.[41] Placental villi from preeclamptic pregnancies show down-regulation of Notch pathway members.[42] Notch signalling in placenta has been suggested to play a role in the development of preeclampsia,[42, 43] and the altered expression of DTX and HES1 in tissue from preeclamptic pregnancies as compared to normal pregnancies, are presented for the first time.

In summary, we have provided a comprehensive transcriptional profile of the decidua in preeclampsia. Our network analysis has demonstrated extensive connectivity between the differently expressed genes. Alteration of the expression level of one gene may influence the transcription of others included in the network. Due to this, it is difficult to pin-point the genes having primary roles in perpetuating preeclampsia from our data set. Some of our findings confirm and elaborate the current knowledge on the pathophysiology of preeclampsia, while others are novel. Further studies are warranted to replicate findings and confirm involvement of specific genes that have been identified.

Acknowledgments

This work was supported by grants from The Norwegian University of Science and Technology (NTNU) (Mari Løset, Siv B. Mundal and Rigmor Austgulen), the Central Norway Regional Health Authority (Mona H. Fenstad), the Research Council of Norway (Mona H. Fenstad), the Fulbright Foundation for Educational Exchange (Mona H. Fenstad), National Institutes of Health grants R01 HD049847 (Eric K. Moses, John Blangero) and R01 MH059490 (John Blangero) and a grant from the Southwest Foundation Forum (Matthew P. Johnson). This investigation was conducted, in part, in facilities constructed with support for the Research Facilities Improvement Program grant C06 RR017515 from the National Center for Research Resources, National Institute of Health.

We thank all the delivering mothers whose participation made this work possible. We are grateful for the statistical expertise at Southwest Foundation for Biomedical Research, San Antonio, TX: Drs Jac C. Charlesworth and Thomas D. Dyer, and at the Norwegian University of Science and Technology, Trondheim, Norway: Dr Åsa

Johansson and Jostein Johannesen at the FUGE bioinformatics platform. We thank Dr Linda Tømmerdal Roten for her valuable advice and comments made during the manuscript preparation.

References

1. Redman CW, Sargent IL. Placental stress and pre-eclampsia: a revised view. Placenta 2009;30 (Suppl A):S38–42. [PubMed: 19138798]
2. Hung TH, Burton GJ. Hypoxia and reoxygenation: a possible mechanism for placental oxidative stress in preeclampsia. Taiwan J Obstet Gynecol 2006;45:189–200. [PubMed: 17175463]
3. Staff AC, Halvorsen B, Ranheim T, et al. Elevated level of free 8-iso-prostaglandin F2alpha in the decidua basalis of women with preeclampsia. Am J Obstet Gynecol 1999;181:1211–5. [PubMed: 10561647]
4. Staff AC, Ranheim T, Khoury J, et al. Increased contents of phospholipids, cholesterol, and lipid peroxides in decidua basalis in women with preeclampsia. Am J Obstet Gynecol 1999;180:587–92. [PubMed: 10076133]
5. Salonen Ros H, Lichtenstein P, Lipworth L, et al. Genetic effects on the liability of developing pre-eclampsia and gestational hypertension. Am J Med Genet 2000;91:256–60. [PubMed: 10766979]
6. Moses EK, Fitzpatrick E, Freed KA, et al. Objective prioritization of positional candidate genes at a quantitative trait locus for pre-eclampsia on 2q22. Mol Hum Reprod 2006;12:505–12. [PubMed: 16809377]
7. Lie RT, Rasmussen S, Brunborg H, et al. Fetal and maternal contributions to risk of pre-eclampsia: population based study. BMJ 1998;316:1343–7. [PubMed: 9563982]
8. Schadt EE, Zhang B, Zhu J. Advances in systems biology are enhancing our understanding of disease and moving us closer to novel disease treatments. Genetica 2009;136:259–69. [PubMed: 19363597]
9. Founds SA, Dorman JS, Conley YP. Microarray technology applied to the complex disorder of preeclampsia. J Obstet Gynecol Neonatal Nurs 2008;37:146–57.
10. Winn VD, Gormley M, Paquet AC, et al. Severe preeclampsia-related changes in gene expression at the maternal-fetal interface include sialic acid-binding immunoglobulin-like lectin-6 and pappalysin-2. Endocrinology 2009;150:452–62. [PubMed: 18818296]
11. Herse F, Dechend R, Harsem NK, et al. Dysregulation of the circulating and tissue-based renin-angiotensin system in preeclampsia. Hypertension 2007;49:604–11. [PubMed: 17261642]
12. Gifford RW, August PA, Cunningham G, et al. Report of the National High Blood Pressure Education Program Working Group on High Blood Pressure in Pregnancy. Am J Obstet Gynecol 2000;183:S1–S22.
13. Harsem NK, Staff AC, He L, et al. The decidual suction method: a new way of collecting decidual tissue for functional and morphological studies. Acta Obstet Gynecol Scand 2004;83:724–30. [PubMed: 15255844]
14. Almasy L, Blangero J. Multipoint quantitative-trait linkage analysis in general pedigrees. Am J Hum Genet 1998;62:1198–211. [PubMed: 9545414]
15. Goring HH, Curran JE, Johnson MP, et al. Discovery of expression QTLs using large-scale transcriptional profiling in human lymphocytes. Nat Genet 2007;39:1208–16. [PubMed: 17873875]
16. Livak KJ, Schmittgen TD. Analysis of relative gene expression data using real-time quantitative PCR and the 2(-Delta Delta C(T)) Method. Methods 2001;25:402–8. [PubMed: 11846609]
17. Hellemans J, Mortier G, De Paepe A, et al. qBase relative quantification framework and software for management and automated analysis of real-time quantitative PCR data. Genome Biol 2007;8:R19. [PubMed: 17291332]
18. Benjamini Y, Hochberg Y. Controlling the false discovery rate: a practical and powerful approach to multiple testing. J R Stat Soc 1995;57:289–300.
19. Gentleman RC, Carey VJ, Bates DM, et al. Bioconductor: open software development for computational biology and bioinformatics. Genome Biol 2004;5:R80. [PubMed: 15461798]

20. Staff AC, Ranheim T, Halvorsen B. Augmented PLA2 activity in pre-eclamptic decidual tissue--a key player in the pathophysiology of 'acute atherosis' in pre-eclampsia? Placenta 2003;24:965–73. [PubMed: 14580379]
21. Enquobahrie DA, Meller M, Rice K, et al. Differential placental gene expression in preeclampsia. Am J Obstet Gynecol 2008;199:566, e1–11. [PubMed: 18533121]
22. Ahmed A, Rahman M, Zhang X, et al. Induction of placental heme oxygenase-1 is protective against TNFalpha-induced cytotoxicity and promotes vessel relaxation. Mol Med 2000;6:391–409. [PubMed: 10952020]
23. Winn VD, Haimov-Kochman R, Paquet AC, et al. Gene expression profiling of the human maternal-fetal interface reveals dramatic changes between midgestation and term. Endocrinology 2007;148:1059–79. [PubMed: 17170095]
24. Mikheev AM, Nabekura T, Kaddoumi A, et al. Profiling gene expression in human placentae of different gestational ages: an OPRU Network and UW SCOR Study. Reprod Sci 2008;15:866–77. [PubMed: 19050320]
25. Ackermann M, Strimmer K. A general modular framework for gene set enrichment analysis. BMC Bioinformatics 2009;10:47. [PubMed: 19192285]
26. Carlson MR, Zhang B, Fang Z, et al. Gene connectivity, function, and sequence conservation: predictions from modular yeast co-expression networks. BMC Genomics 2006;7:40. [PubMed: 16515682]
27. Gawrieh S, Baye TM, Carless M, et al. Hepatic Gene Networks in Morbidly Obese Patients With Nonalcoholic Fatty Liver Disease. Obes Surg. 2010
28. Kudo Y, Boyd CA, Sargent IL, et al. Decreased tryptophan catabolism by placental indoleamine 2,3-dioxygenase in preeclampsia. Am J Obstet Gynecol 2003;188:719–26. [PubMed: 12634647]
29. Santoso DI, Rogers P, Wallace EM, et al. Localization of indoleamine 2,3-dioxygenase and 4-hydroxynonenal in normal and pre-eclamptic placentae. Placenta 2002;23:373–9. [PubMed: 12061852]
30. Opitz CA, Wick W, Steinman L, et al. Tryptophan degradation in autoimmune diseases. Cell Mol Life Sci 2007;64:2542–63. [PubMed: 17611712]
31. Burton GJ, Yung HW, Cindrova-Davies T, et al. Placental endoplasmic reticulum stress and oxidative stress in the pathophysiology of unexplained intrauterine growth restriction and early onset preeclampsia. Placenta 2009;30 (Suppl A):S43–8. [PubMed: 19081132]
32. Yung HW, Calabrese S, Hynx D, et al. Evidence of placental translation inhibition and endoplasmic reticulum stress in the etiology of human intrauterine growth restriction. Am J Pathol 2008;173:451–62. [PubMed: 18583310]
33. Cullinan SB, Diehl JA. Coordination of ER and oxidative stress signaling: the PERK/Nrf2 signaling pathway. Int J Biochem Cell Biol 2006;38:317–32. [PubMed: 16290097]
34. Itoh K, Chiba T, Takahashi S, et al. An Nrf2/small Maf heterodimer mediates the induction of phase II detoxifying enzyme genes through antioxidant response elements. Biochem Biophys Res Commun 1997;236:313–22. [PubMed: 9240432]
35. De Wolf F, Robertson WB, Brosens I. The ultrastructure of acute atherosis in hypertensive pregnancy. Am J Obstet Gynecol 1975;123:164–74. [PubMed: 1163579]
36. Branch DW, Mitchell MD, Miller E, et al. Pre-eclampsia and serum antibodies to oxidised low-density lipoprotein. Lancet 1994;343:645–6. [PubMed: 7509433]
37. Walsh SW. Maternal-placental interactions of oxidative stress and antioxidants in preeclampsia. Semin Reprod Endocrinol 1998;16:93–104. [PubMed: 9654611]
38. Hubel CA, Roberts JM, Taylor RN, et al. Lipid peroxidation in pregnancy: new perspectives on preeclampsia. Am J Obstet Gynecol 1989;161:1025–34. [PubMed: 2679100]
39. Artavanis-Tsakonas S, Rand MD, Lake RJ. Notch signaling: cell fate control and signal integration in development. Science 1999;284:770–6. [PubMed: 10221902]
40. Liu ZJ, Shirakawa T, Li Y, et al. Regulation of Notch1 and Dll4 by vascular endothelial growth factor in arterial endothelial cells: implications for modulating arteriogenesis and angiogenesis. Mol Cell Biol 2003;23:14–25. [PubMed: 12482957]
41. De Falco M, Cobellis L, Giraldi D, et al. Expression and distribution of notch protein members in human placenta throughout pregnancy. Placenta 2007;28:118–26. [PubMed: 17185135]

42. Cobellis L, Mastrogiacomo A, Federico E, et al. Distribution of Notch protein members in normal and preeclampsia-complicated placentas. Cell Tissue Res 2007;330:527–34. [PubMed: 17955263]

43. Sitras V, Paulssen RH, Gronaas H, et al. Differential placental gene expression in severe preeclampsia. Placenta 2009;30:424–33. [PubMed: 19249095]

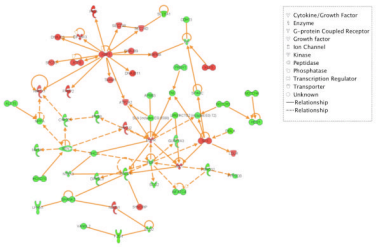

FIGURE I.

The Ingenuity Pathway Analysis (Ingenuity Systems, www.ingenuity.com) generated gene/gene product interaction network of preeclampsia correlated genes. Genes or gene products are represented as nodes, and the biological relationship between two nodes is represented as an edge (line). All edges are supported by at least one published reference. Solid edges represent a direct relationship and dashed edges represent an indirect relationship. Node color represents the correlation of expression level with preeclampsia, and the color intensity indicates the degree of correlation (red is positive and green negative). The shape of each node represents the functional class of the gene product, as shown in the key.

TABLE 1

Clinical characteristics of study groups

Variable	[a] Preeclamptic pregnancies (n = 37)	[a] Normal pregnancies (n = 58)
Gestational age (wk)	32 ± 4[b]	39 ± 1
Systolic blood pressure (mm Hg)	152 ± 16[b]	116 ± 10
Diastolic blood pressure (mm Hg)	96 ± 10[b]	70 ± 9.0
Birthweight (g)	1555 ± 769[b]	3619 ± 469
Body mass index (kg/m^2)[c]	27.7 ± 6.2	25.3 ± 5.7

Values are means ± SD.

[a] 43 women with pregnancies complicated by preeclampsia and 59 women with normal pregnancies were included in the study. Six samples from preeclamptic pregnancies and one sample from a normal pregnancy were excluded from gene expression analysis due to low RNA quality.

[b] P <0.001 obtained with t-test statistics with SPSS software (version 16; SPSS Inc, Chicago, IL).

[c] Body mass index was measured at first antenatal care visit.

TABLE 2

Differentially expressed transcripts[a]

Illumina ID	GenBank ID	Symbol	Definition	Ch	[b] Beta value	[c] *P* value	[d] FDR *P* value
ILMN_1782259	NM_173078.2	SLITRK4	SLIT and NTRK-like family, member 4	X	−1.0363	4.6×10^{-8}	0.0012
ILMN_1680465	NM_178815.3	ARL5B	ADP-ribosylation factor-like 5B	10	0.9122	4.5×10^{-7}	0.0039
ILMN_1743367	NM_012193.2	FZD4	frizzled homolog 4 (Drosophila)	11	−0.9122	4.1×10^{-7}	0.0054
ILMN_1726210	NM_178172.2	LOC338328	high density lipoprotein-binding protein	8	−0.8672	3.7×10^{-6}	0.0088
ILMN_1709222	NM_005692.3	ABCF2	ATP-binding cassette, sub-family F (GCN20), member 2, nuclear gene encoding mitochondrial protein, transcript variant 2	7	−0.8634	3.5×10^{-6}	0.0093
ILMN_1772612	NM_012098.2	ANGPTL2	angiopoietin-like 2	9	−0.8884	4.4×10^{-6}	0.0097
ILMN_1659792	NM_014213.2	HOXD9	homeobox D9	2	−0.8541	3.5×10^{-6}	0.0102
ILMN_1813295	NM_018640.3	LMO3	LIM domain only 3 (rhombotin-like 2), transcript variant 1	12	−0.8992	3.3×10^{-6}	0.0110
ILMN_1669023	NM_020482.3	FHL5	four and a half LIM domains 5	6	−0.8489	3.2×10^{-6}	0.0123
ILMN_1658677	NM_178502.2	DTX3	deltex 3 homolog (Drosophila)	12	−0.9038	2.9×10^{-6}	0.0130
ILMN_1812461	NM_003881.2	WISP2	WNT1 inducible signaling pathway protein 2	20	−0.8717	6.6×10^{-6}	0.0134
ILMN_1776157	NM_080415.1	SEPT4	septin 4, transcript variant 2	17	−0.8882	2.6×10^{-6}	0.0140
ILMN_1794370	NM_001031702.2	SEMA5B	sema domain, seven thrombospondin repeats (type 1 and type 1-like), transmembrane domain (TM) and short cytoplasmic domain, (semaphorin) 5B, transcript variant 1	3	−0.8695	8.0×10^{-6}	0.0141
ILMN_1719069	NM_213596.1	FOXN4	forkhead box N4	12	−0.8803	7.8×10^{-6}	0.0147
ILMN_1733667	NM_021931.2	DHX35	DEAH (Asp-Glu-Ala-His) box polypeptide 35	20	−0.8537	9.0×10^{-6}	0.0149
ILMN_1734276	NM_199169.1	TMEPAI	transmembrane, prostate androgen induced RNA, transcript variant 2	20	−0.8360	1.6×10^{-5}	0.0153
ILMN_1701195	NM_005084.2	PLA2G7	phospholipase A2, group VII (platelet-activating factor acetylhydrolase, plasma)	6	0.8305	1.6×10^{-5}	0.0155
ILMN_1687821	NM_033201.1	C16orf45	chromosome 16 open reading frame 45	16	−0.8218	1.4×10^{-5}	0.0156
ILMN_1736911	NM_003275.2	TMOD1	tropomodulin 1	9	−0.8178	1.5×10^{-5}	0.0157
ILMN_1744487	NM_015645.2	C1QTNF5	C1q and tumor necrosis factor related protein 5	11	−0.8113	1.7×10^{-5}	0.0157
ILMN_1767556	NM_007021.2	C10orf10	chromosome 10 open reading frame 10	10	−0.7966	1.3×10^{-5}	0.0158
ILMN_1668249	NM_022773.2	TMEM112	transmembrane protein 112	16	−0.8079	1.6×10^{-5}	0.0158
ILMN_1788462	NM_001033059.1	AMD1	adenosylmethionine decarboxylase 1, transcript variant 2	6	0.8027	1.4×10^{-5}	0.0160
ILMN_1665945	NM_022735.3	ACBD3	acyl-Coenzyme A binding domain containing 3	1	0.8297	1.3×10^{-5}	0.0164
ILMN_1657803	NM_001014975.1	CFH	complement factor H, transcript variant 2	1	−0.8780	2.5×10^{-6}	0.0164

Illumina ID	GenBank ID	Symbol	Definition	Ch	[b] Beta value	[c] *P* value	[d] FDR *P* value
ILMN_1880012	NM_003966.2	SEMA5A	sema domain, seven thrombospondin repeats (type 1 and type 1-like), transmembrane domain (TM) and short cytoplasmic domain, (semaphorin) 5A	5	0.8208	2.7×10^{-5}	0.0168
ILMN_1763036	NM_001286.2	CLCN6	chloride channel 6, transcript variant ClC-6a	1	−0.8027	2.4×10^{-5}	0.0170
ILMN_1710962	NM_014573.2	TMEM97	transmembrane protein 97	17	0.8236	2.6×10^{-5}	0.0171
ILMN_1801927	NM_001004311.2	FIGLA	folliculogenesis specific basic helix-loop-helix	2	−0.8616	1.1×10^{-5}	0.0171
ILMN_1673773	NM_198516.1	GALNTL4	UDP-N-acetyl-alpha-D-galactosamine:polypeptide N-acetylgalactosaminyltransferase-like 4	11	−0.7998	2.3×10^{-5}	0.0172
ILMN_1711516	NM_001690.2	ATP6V1A	ATPase, H+ transporting, lysosomal 70kDa, V1 subunit A	3	0.8101	1.2×10^{-5}	0.0172
ILMN_1715555	NM_001352.2	DBP	D site of albumin promoter (albumin D-box) binding protein	19	−0.7916	1.3×10^{-5}	0.0172
ILMN_1779632	NM_001001723.1	TMEM1	transmembrane protein 1, transcript variant 2	21	0.8054	2.6×10^{-5}	0.0172
ILMN_1685703	NM_003500.2	ACOX2	acyl-Coenzyme A oxidase 2, branched chain	3	−0.8253	2.2×10^{-5}	0.0173
ILMN_1711157	NM_004557.3	NOTCH4	Notch homolog 4 (Drosophila)	6	−0.7709	2.5×10^{-5}	0.0174
ILMN_1740160	NM_182811.1	PLCG1	phospholipase C, gamma 1, transcript variant 2	20	−0.8077	2.1×10^{-5}	0.0176
ILMN_1834017	N25708	Hs.573236	yx79f04s1 Soares melanocyte 2NbHM cDNA clone IMAGE:267967 3 sequence		0.8058	2.3×10^{-5}	0.0176
ILMN_1798076	NM_006898.4	HOXD3	homeobox D3	2	−0.8238	2.3×10^{-5}	0.0176
ILMN_1705985	NM_020473.2	PIGA	phosphatidylinositol glycan anchor biosynthesis, class A (paroxysmal nocturnal hemoglobinuria), transcript variant 3	X	0.7983	2.6×10^{-5}	0.0177
ILMN_1772302	NM_006441.1	MTHFS	5,10-methenyltetrahydrofolate synthetase (5-formyltetrahydrofolate cyclo-ligase)	15	0.7802	2.9×10^{-5}	0.0178
ILMN_1781791	NM_000950.1	PRRG1	proline rich Gla (G-carboxyglutamic acid) 1	X	0.7681	3.2×10^{-5}	0.0179
ILMN_1748812	NM_152913.1	TMEM130	transmembrane protein 130	7	−0.7814	3.0×10^{-5}	0.0179
ILMN_1680774	XM_001132373.1	LOC730994	similar to NACHT, leucine rich repeat and PYD (pyrin domain) containing 1, transcript variant 1	17	−0.8034	2.0×10^{-5}	0.0179
ILMN_1755120	NM_006699.3	MAN1A2	mannosidase, alpha, class 1A, member 2	1	0.8519	1.3×10^{-5}	0.0180
ILMN_1788166	NM_003318.3	TTK	TTK protein kinase	6	0.8169	2.1×10^{-5}	0.0181
ILMN_1685608	NM_002523.1	NPTX2	neuronal pentraxin II	7	−0.7865	3.1×10^{-5}	0.0181
ILMN_1678842	NM_003247.2	THBS2	thrombospondin 2	6	−0.8054	3.2×10^{-5}	0.0182
ILMN_1813430	NM_182985.3	TRIM69	tripartite motif-containing 69, transcript variant a	15	−0.8120	3.5×10^{-5}	0.0192
ILMN_1675936	NM_016438.2	HIGD1B	HIG1 domain family, member 1B	17	−0.8060	3.9×10^{-5}	0.0202
ILMN_1877909	BX105647	Hs.125533	BX105647 Soares_NFL_T_GBC_S1 cDNA clone IMAGp998F143713 sequence		−0.7992	3.7×10^{-5}	0.0202
ILMN_1803279	NM_016040.3	TMED5	transmembrane emp24 protein transport domain containing 5	1	0.7904	3.8×10^{-5}	0.0202
ILMN_1700202	NM_022918.2	TMEM135	transmembrane protein 135	11	0.7615	4.1×10^{-5}	0.0206
ILMN_1727589	NM_004605.2	SULT2B1	sulfotransferase family, cytosolic, 2B, member 1, transcript variant 1	19	0.7826	4.2×10^{-5}	0.0209

Illumina ID	GenBank ID	Symbol	Definition	Ch	[b] Beta value	[c] *P* value	[d] FDR *P* value
ILMN_1811873	NM_002889.2	RARRES2	retinoic acid receptor responder (tazarotene induced) 2	7	−0.7690	4.4×10^{-5}	0.0214
ILMN_1703955	NM_148177.1	FBXO32	F-box protein 32, transcript variant 2	8	−0.8049	4.8×10^{-5}	0.0225
ILMN_1731358	NM_018181.4	ZNF532	zinc finger protein 532	18	−0.7974	4.7×10^{-5}	0.0226
ILMN_1682937	NM_001038633.2	RSPO1	R-spondin homolog (Xenopus laevis)	1	−0.7973	5.0×10^{-5}	0.0230
ILMN_1695947	NM_174934.2	SCN4B	sodium channel, voltage-gated, type IV, beta	11	−0.7948	5.8×10^{-5}	0.0234
ILMN_1707342	NM_015541.2	LRIG1	leucine-rich repeats and immunoglobulin-like domains 1	3	−0.7679	5.8×10^{-5}	0.0235
ILMN_1781626	NM_001734.2	C1S	complement component 1, s subcomponent, transcript variant 1	12	−0.7833	5.7×10^{-5}	0.0236
ILMN_1676215	NM_001364.2	DLG2	discs, large homolog 2, chapsyn-110 (Drosophila)	11	−0.7928	5.6×10^{-5}	0.0238
ILMN_1880210	BC038188	Hs.179213	Homo sapiens, clone IMAGE:3451765		0.7666	5.7×10^{-5}	0.0239
ILMN_1767225	NM_006092.1	NOD1	nucleotide-binding oligomerization domain containing 1	7	−0.7808	5.3×10^{-5}	0.0239
ILMN_1793410	NM_021021.2	SNTB1	syntrophin, beta 1 (dystrophin-associated protein A1, 59kDa, basic component 1)	8	0.7636	5.5×10^{-5}	0.0239
ILMN_1752837	NM_018184.2	ARL8B	ADP-ribosylation factor-like 8B	3	0.7644	5.3×10^{-5}	0.0241
ILMN_1791949	NM_032507.2	PGBD1	piggyBac transposable element derived 1	6	−0.7478	5.5×10^{-5}	0.0243
ILMN_1859863	BM458075	Hs.555181	AGENCOURT_6411402 NIH_MGC_71 cDNA clone IMAGE:5530423 5 sequence		0.7667	6.4×10^{-5}	0.0248
ILMN_1782788	NM_003651.3	CSDA	cold shock domain protein A	12	−0.7756	6.3×10^{-5}	0.0251
ILMN_1727740	NM_006372.3	SYNCRIP	synaptotagmin binding, cytoplasmic RNA interacting protein	6	0.6949	6.7×10^{-5}	0.0253
ILMN_1677396	NM_019080.1	NDFIP2	Nedd4 family interacting protein 2	13	0.7591	6.6×10^{-5}	0.0253
ILMN_1744191	NM_003042.2	SLC6A1	solute carrier family 6 (neurotransmitter transporter, GABA), member 1	3	−0.7914	6.9×10^{-5}	0.0253
ILMN_1656129	NM_020342.1	SLC39A10	solute carrier family 39 (zinc transporter), member 10	2	0.7306	6.8×10^{-5}	0.0253
ILMN_1809639	NM_178505.5	TMEM26	transmembrane protein 26	10	0.7732	7.9×10^{-5}	0.0287
ILMN_1786326	NM_024076.1	KCTD15	potassium channel tetramerisation domain containing 15	19	−0.7853	8.2×10^{-5}	0.0291
ILMN_1651343	NM_001004439.1	ITGA11	integrin, alpha 11	15	−0.7812	8.2×10^{-5}	0.0292
ILMN_1739887	NM_031491.2	RBP5	retinol binding protein 5, cellular	12	−0.7607	8.7×10^{-5}	0.0304
ILMN_1716247	NM_203371.1	FIBIN	fin bud initiation factor	11	−0.7760	8.9×10^{-5}	0.0307
ILMN_1752668	NM_015345.2	DAAM2	dishevelled associated activator of morphogenesis 2	6	−0.7617	1.0×10^{-4}	0.0309
ILMN_1789243	NM_018668.3	VPS33B	vacuolar protein sorting 33 homolog B (yeast)	15	−0.7368	1.0×10^{-4}	0.0312
ILMN_1763852	NM_001093.3	ACACB	acetyl-Coenzyme A carboxylase beta	12	−0.7651	9.6×10^{-5}	0.0314
ILMN_1731561	NM_022370.2	ROBO3	roundabout, axon guidance receptor, homolog 3 (Drosophila)	11	−0.7335	1.0×10^{-4}	0.0314
ILMN_1672635	NM_182947.2	GEFT	RhoA/RAC/CDC42 exchange factor, transcript variant 1	12	−0.7711	9.3×10^{-5}	0.0315

Illumina ID	GenBank ID	Symbol	Definition	Ch	[b] Beta value	[c] *P* value	[d] FDR *P* value
ILMN_1691181	NM_030755.4	TXNDC1	thioredoxin domain containing 1	14	0.7498	1.1×10^{-4}	0.0315
ILMN_1742034	NM_000261.1	MYOC	myocilin, trabecular meshwork inducible glucocorticoid response	1	−0.7416	1.0×10^{-4}	0.0315
ILMN_1761968	NM_033256.1	PPP1R14A	protein phosphatase 1, regulatory (inhibitor) subunit 14A	19	−0.7785	9.5×10^{-5}	0.0315
ILMN_1703142	NM_001005416.1	MARCH2	membrane-associated ring finger (C3HC4) 2, transcript variant 3	19	−0.7337	1.0×10^{-4}	0.0316
ILMN_1752225	NR_002330.1	ST7OT1	ST7 overlapping transcript 1 (antisense non-coding RNA)	7	−0.7606	9.8×10^{-5}	0.0318
ILMN_1667692	NM_000961.3	PTGIS	prostaglandin I2 (prostacyclin) synthase	20	−0.7787	9.5×10^{-5}	0.0318
ILMN_1691457	NM_004900.3	APOBEC3B	apolipoprotein B mRNA editing enzyme, catalytic polypeptide-like 3B	22	0.7343	1.0×10^{-4}	0.0319
ILMN_1728979	NM_207310.1	CCDC74B	coiled-coil domain containing 74B	2	−0.7428	1.2×10^{-4}	0.0320
ILMN_1688346	NM_176814.3	ZNF800	zinc finger protein 800	7	0.7259	1.2×10^{-4}	0.0323
ILMN_1682428	NM_144584.1	C1orf59	chromosome 1 open reading frame 59	1	0.7635	1.2×10^{-4}	0.0323
ILMN_1755173	NM_020904.1	PLEKHA4	pleckstrin homology domain containing, family A (phosphoinositide binding specific) member 4	19	−0.7470	1.1×10^{-4}	0.0324
ILMN_1782954	NM_005339.3	UBE2K	ubiquitin-conjugating enzyme E2-25K	4	0.7190	1.2×10^{-4}	0.0324
ILMN_1735996	NM_016931.2	NOX4	NADPH oxidase 4	11	−0.7504	1.3×10^{-4}	0.0325
ILMN_1680110	NM_006829.2	C10orf116	chromosome 10 open reading frame 116	10	−0.7497	1.2×10^{-4}	0.0325
ILMN_1755832	NM_000435.2	NOTCH3	Notch homolog 3 (Drosophila)	19	−0.7589	1.1×10^{-4}	0.0325
ILMN_1800463	NM_017859.2	UCKL1	uridine-cytidine kinase 1-like 1	20	−0.7338	1.2×10^{-4}	0.0326
ILMN_1674337	NM_004470.2	FKBP2	FK506 binding protein 2, 13kDa, transcript variant 1	11	0.7401	1.2×10^{-4}	0.0327
ILMN_1807171	NM_000929.2	PLA2G5	phospholipase A2, group V	1	−0.7349	1.3×10^{-4}	0.0327
ILMN_1724671	NM_207577.1	MAP6	microtubule-associated protein 6, transcript variant 2	11	−0.7623	1.2×10^{-4}	0.0328
ILMN_1655117	NM_025132.3	WDR19	WD repeat domain 19	4	−0.7425	1.3×10^{-4}	0.0328
ILMN_1706511	NM_003216.2	TEF	thyrotrophic embryonic factor	22	−0.7288	1.1×10^{-4}	0.0328
ILMN_1677018	NM_002141.4	HOXA4	homeobox A4	7	−0.7424	1.3×10^{-4}	0.0333
ILMN_1785646	NM_153321.1	PMP22	peripheral myelin protein 22, transcript variant 2	17	−0.7487	1.3×10^{-4}	0.0334
ILMN_1709661	NM_145276.1	ZNF563	zinc finger protein 563	19	−0.7481	1.4×10^{-4}	0.0334
ILMN_1736863	NM_018295.2	TMEM140	transmembrane protein 140	7	−0.7336	1.3×10^{-4}	0.0337
ILMN_1807379	NM_023034.1	WHSC1L1	Wolf-Hirschhorn syndrome candidate 1-like 1, transcript variant long	8	0.7237	1.4×10^{-4}	0.0338
ILMN_1740842	NM_005407.1	SALL2	sal-like 2 (Drosophila)	14	−0.7458	1.4×10^{-4}	0.0340
ILMN_1734229	NM_032802.3	SPPL2A	signal peptide peptidase-like 2A	15	0.7168	1.4×10^{-4}	0.0343
ILMN_1696003	NM_006496.1	GNAI3	guanine nucleotide binding protein (G protein), alpha inhibiting activity polypeptide 3	1	0.7101	1.5×10^{-4}	0.0343

Illumina ID	GenBank ID	Symbol	Definition	Ch	[b] Beta value	[c] *P* value	[d] FDR *P* value
ILMN_1793770	NM_058246.3	DNAJB6	DnaJ (Hsp40) homolog, subfamily B, member 6, transcript variant 1	7	−0.7448	1.4×10^{-4}	0.0343
ILMN_1797861	NM_002184.2	IL6ST	interleukin 6 signal transducer (gp130, oncostatin M receptor), transcript variant 1	5	0.7406	1.6×10^{-4}	0.0353
ILMN_1720865	NM_145798.2	OSBPL7	oxysterol binding protein-like 7, transcript variant 1	17	−0.7298	1.6×10^{-4}	0.0355
ILMN_1713978	NM_006923.2	SDF2	stromal cell-derived factor 2	17	0.7243	1.6×10^{-4}	0.0356
ILMN_1682231	NM_001003682.2	TTMB	TTMB protein	1	−0.7581	1.6×10^{-4}	0.0356
ILMN_1684554	NM_001856.3	COL16A1	collagen, type XVI, alpha 1	1	−0.7316	1.5×10^{-4}	0.0356
ILMN_1778595	NM_003063.2	SLN	sarcolipin	11	−0.7375	1.6×10^{-4}	0.0356
ILMN_1811790	NM_004118.3	FKHL18	forkhead-like 18 (Drosophila)	20	−0.7197	1.6×10^{-4}	0.0357
ILMN_1712461	NM_004352.1	CBLN1	cerebellin 1 precursor	16	−0.7413	1.5×10^{-4}	0.0358
ILMN_1815874	NM_018946.2	NANS	N-acetylneuraminic acid synthase (sialic acid synthase)	9	0.7205	1.7×10^{-4}	0.0359
ILMN_1720819	XM_934796.2	LOC653566	similar to Signal peptidase complex subunit 2 (Microsomal signal peptidase 25 kDa subunit) (SPase 25 kDa subunit), transcript variant 3	1	0.6515	1.7×10^{-4}	0.0359
ILMN_1669898	NM_201446.1	EGFL7	EGF-like-domain, multiple 7, transcript variant 2	9	−0.6935	1.5×10^{-4}	0.0359
ILMN_1740441	NM_000398.4	CYB5R3	cytochrome b5 reductase 3, transcript variant M	22	−0.7263	1.7×10^{-4}	0.0360
ILMN_1700274	NM_031442.2	TMEM47	transmembrane protein 47	X	−0.7303	1.6×10^{-4}	0.0360
ILMN_1720889	NM_001017369.1	SC4MOL	sterol-C4-methyl oxidase-like, transcript variant 2	4	0.6822	1.7×10^{-4}	0.0367
ILMN_1793543	NM_144697.2	C1orf51	chromosome 1 open reading frame 51	1	−0.7115	1.8×10^{-4}	0.0376
ILMN_1734288	NM_152511.3	DUSP18	dual specificity phosphatase 18	22	−0.7243	1.9×10^{-4}	0.0383
ILMN_1678998	NM_014665.1	LRRC14	leucine rich repeat containing 14	8	−0.7119	1.9×10^{-4}	0.0383
ILMN_1791508	NM_024302.3	MMP28	matrix metallopeptidase 28, transcript variant 1	17	−0.7246	1.9×10^{-4}	0.0385
ILMN_1688295	NM_016423.1	ZNF219	zinc finger protein 219	14	−0.7437	1.9×10^{-4}	0.0388
ILMN_1770293	NM_001730.3	KLF5	Kruppel-like factor 5 (intestinal)	13	0.7122	1.9×10^{-4}	0.0388
ILMN_1886424	BG621061	Hs.559870	602616941F1 NIH_MGC_79 cDNA clone IMAGE:4730410 5 sequence		−0.7236	1.9×10^{-4}	0.0388
ILMN_1697006	XM_930748.2	LOC642361	hypothetical protein LOC642361	10	−0.6926	2.2×10^{-4}	0.0400
ILMN_1673543	NM_018290.2	PGM2	phosphoglucomutase 2	4	0.6845	2.0×10^{-4}	0.0401
ILMN_1742230	NM_182648.1	BAZ1A	bromodomain adjacent to zinc finger domain, 1A, transcript variant 2	14	0.7376	2.1×10^{-4}	0.0401
ILMN_1659843	NM_006260.2	DNAJC3	DnaJ (Hsp40) homolog, subfamily C, member 3	13	0.7094	2.1×10^{-4}	0.0401
ILMN_1696585	NM_017671.4	C20orf42	chromosome 20 open reading frame 42	20	0.7335	2.1×10^{-4}	0.0402
ILMN_1763641	NM_025040.2	ZNF614	zinc finger protein 614	19	0.7013	2.1×10^{-4}	0.0402

Illumina ID	GenBank ID	Symbol	Definition	Ch	[b] Beta value	[c] *P* value	[d] FDR *P* value
ILMN_1726678	NM_014147.1	HSPC047	HSPC047 protein	7	−0.7153	2.0×10^{-4}	0.0402
ILMN_1779034	NM_018161.4	NADSYN1	NAD synthetase 1	11	−0.6854	2.1×10^{-4}	0.0402
ILMN_1705253	NM_130393.2	PTPRD	protein tyrosine phosphatase, receptor type, D, transcript variant 4	9	0.7342	2.1×10^{-4}	0.0403
ILMN_1837017	CB269825	Hs.543359	1008732 Human Fat Cell 5-Stretch Plus cDNA Library cDNA 5′ sequence		−0.7281	2.1×10^{-4}	0.0405
ILMN_1829490	BX106357	Hs.445732	BX106357 Soares_NFL_T_GBC_S1 cDNA clone IMAGp998B055155 sequence		0.6957	2.2×10^{-4}	0.0409
ILMN_1714691	NM_002148.3	HOXD10	homeobox D10	2	−0.7265	2.3×10^{-4}	0.0413
ILMN_1803213	NM_015419.2	MXRA5	matrix-remodelling associated 5	X	−0.7061	2.3×10^{-4}	0.0416
ILMN_1732158	NM_001460.2	FMO2	flavin containing monooxygenase 2 (non-functional)	1	−0.6950	2.4×10^{-4}	0.0424
ILMN_1681938	NM_022568.2	ALDH8A1	aldehyde dehydrogenase 8 family, member A1, transcript variant 1	6	0.6875	2.4×10^{-4}	0.0424
ILMN_1753243	NM_016306.4	DNAJB11	DnaJ (Hsp40) homolog, subfamily B, member 11	3	0.7183	2.5×10^{-4}	0.0431
ILMN_1793846	NM_014670.2	BZW1	basic leucine zipper and W2 domains 1	2	0.7033	2.7×10^{-4}	0.0431
ILMN_1852159	BF753039	Hs.557431	RC3-BN0425-011200-022-c08 BN0425 cDNA sequence		−0.7234	2.4×10^{-4}	0.0432
ILMN_1805992	NM_018330.4	KIAA1598	KIAA1598	10	0.7077	2.4×10^{-4}	0.0433
ILMN_1740512	XM_936687.1	MGC39900	hypothetical protein MGC39900	X	−0.7227	2.6×10^{-4}	0.0433
ILMN_1708916	NM_032512.2	PDZD4	PDZ domain containing 4	X	−0.7075	2.7×10^{-4}	0.0434
ILMN_1773563	NM_015927.3	TGFB1I1	transforming growth factor beta 1 induced transcript 1, transcript variant 2	16	−0.7335	2.6×10^{-4}	0.0435
ILMN_1674184	NM_153022.2	C12orf59	chromosome 12 open reading frame 59	12	0.7122	2.6×10^{-4}	0.0436
ILMN_1657483	NM_032985.4	SEC23B	Sec23 homolog B (S cerevisiae), transcript variant 2	20	0.6717	2.7×10^{-4}	0.0436
ILMN_1772540	NM_015251.2	ASCIZ	ATM/ATR-Substrate Chk2-Interacting Zn2+-finger protein	16	0.6872	2.6×10^{-4}	0.0438
ILMN_1756862	NM_145641.1	APOL3	apolipoprotein L, 3, transcript variant beta/a	22	−0.7021	2.8×10^{-4}	0.0438
ILMN_1685413	NM_024079.4	ALG8	asparagine-linked glycosylation 8 homolog (S cerevisiae, alpha-1,3-glucosyltransferase), transcript variant 1	11	0.6986	2.8×10^{-4}	0.0439
ILMN_1686645	NM_021645.4	UTP14C	UTP14, U3 small nucleolar ribonucleoprotein, homolog C (yeast)	13	0.6746	2.8×10^{-4}	0.0440
ILMN_1813746	NM_003389.2	CORO2A	coronin, actin binding protein, 2A, transcript variant 1	9	0.7135	2.6×10^{-4}	0.0440
ILMN_1765557	NM_015441.1	OLFML2B	olfactomedin-like 2B	1	−0.6714	2.7×10^{-4}	0.0441
ILMN_1740586	NM_000300.2	PLA2G2A	phospholipase A2, group IIA (platelets, synovial fluid)	1	−0.7049	2.6×10^{-4}	0.0443
ILMN_1758750	NR_003501.1	EARS2	glutamyl-tRNA synthetase 2, mitochondrial (putative), transcript variant 2, transcribed RNA	16	0.7199	2.6×10^{-4}	0.0444
ILMN_1703178	NM_003469.3	SCG2	secretogranin II (chromogranin C)	2	−0.7239	2.6×10^{-4}	0.0444
ILMN_1710522	NM_175635.1	RUNX1T1	runt-related transcription factor 1; translocated to, 1 (cyclin D-related), transcript variant 3	8	−0.6886	3.1×10^{-4}	0.0444

Illumina ID	GenBank ID	Symbol	Definition	Ch	[b] Beta value	[c] *P* value	[d] FDR *P* value
ILMN_1730048	NM_024067.2	C7orf26	chromosome 7 open reading frame 26	7	−0.6943	2.9×10^{-4}	0.0444
ILMN_1722855	NM_003377.3	VEGFB	vascular endothelial growth factor B	11	−0.7039	3.0×10^{-4}	0.0445
ILMN_1752915	NM_004124.2	GMFB	glia maturation factor, beta	14	0.6872	2.6×10^{-4}	0.0445
ILMN_1702124	NM_153371.3	LNX2	ligand of numb-protein X 2	13	0.7044	3.0×10^{-4}	0.0445
ILMN_1695299	NM_014476.1	PDLIM3	PDZ and LIM domain 3	4	−0.7140	3.1×10^{-4}	0.0445
ILMN_1666364	NM_144576.3	COQ10A	coenzyme Q10 homolog A (S cerevisiae), transcript variant 1	12	−0.6949	2.6×10^{-4}	0.0445
ILMN_1756942	NM_001017371.3	SP3	Sp3 transcription factor, transcript variant 2	2	0.6849	3.1×10^{-4}	0.0445
ILMN_1750386	NM_006172.2	NPPA	natriuretic peptide precursor A	1	−0.6947	3.1×10^{-4}	0.0445
ILMN_1685433	NM_020351.2	COL8A1	collagen, type VIII, alpha 1, transcript variant 2	3	−0.6900	2.9×10^{-4}	0.0445
ILMN_1665095	NM_015537.3	NELF	nasal embryonic LHRH factor	9	−0.7203	2.9×10^{-4}	0.0445
ILMN_1695316	NM_022154.5	SLC39A8	solute carrier family 39 (zinc transporter), member 8	4	0.6843	2.9×10^{-4}	0.0446
ILMN_1749338	NM_173505.2	ANKRD29	ankyrin repeat domain 29	18	−0.6916	3.0×10^{-4}	0.0446
ILMN_1692340	NM_207404.2	ZNF662	zinc finger protein 662	3	−0.7117	2.9×10^{-4}	0.0447
ILMN_1730612	NM_001048223.1	DBNDD2	dysbindin (dystrobrevin binding protein 1) domain containing 2, transcript variant 3	20	−0.7208	3.1×10^{-4}	0.0447
ILMN_1778523	NM_001206.2	KLF9	Kruppel-like factor 9	9	−0.6988	3.0×10^{-4}	0.0447
ILMN_1813175	NM_014921.3	LPHN1	latrophilin 1, transcript variant 2	19	−0.6905	3.0×10^{-4}	0.0447
ILMN_1800103	XM_001128785.1	LOC731196	similar to Proprotein convertase subtilisin/kexin type 7 precursor (Proprotein convertase PC7) (Subtilisin/kexin-like protease PC7) (Prohormone convertase PC7) (PC8) (hPC8) (Lymphoma proprotein convertase)	11	0.6977	2.9×10^{-4}	0.0447
ILMN_1801583	NM_017680.3	ASPN	asporin	9	−0.7233	2.9×10^{-4}	0.0447
ILMN_1740024	NM_005467.2	NAALAD2	N-acetylated alpha-linked acidic dipeptidase 2	11	−0.6949	3.0×10^{-4}	0.0449
ILMN_1683133	NM_014079.2	KLF15	Kruppel-like factor 15	3	−0.6842	3.2×10^{-4}	0.0451
ILMN_1801441	NM_144629.1	RFTN2	raftlin family member 2	2	−0.6948	3.2×10^{-4}	0.0452
ILMN_1719097	NM_013326.3	C18orf8	chromosome 18 open reading frame 8	18	−0.7098	3.2×10^{-4}	0.0452
ILMN_1723689	NM_003624.1	RANBP3	RAN binding protein 3, transcript variant RANBP3-a	19	−0.6899	3.2×10^{-4}	0.0452
ILMN_1790052	NM_004659.1	MMP23A	matrix metallopeptidase 23A	1	−0.7011	3.3×10^{-4}	0.0456
ILMN_1679262	NM_001387.2	DPYSL3	dihydropyrimidinase-like 3	5	−0.7208	3.3×10^{-4}	0.0458
ILMN_1683487	NM_003444.1	ZNF154	zinc finger protein 154 (pHZ-92)	19	−0.6905	3.3×10^{-4}	0.0460
ILMN_1710284	NM_005524.2	HES1	hairy and enhancer of split 1, (Drosophila)	3	−0.7019	3.4×10^{-4}	0.0462
ILMN_1728710	NM_001031665.1	ZNF816A	zinc finger protein 816A	19	0.6975	3.5×10^{-4}	0.0462

Illumina ID	GenBank ID	Symbol	Definition	Ch	[b] Beta value	[c] *P* value	[d] FDR *P* value
ILMN_1685156	NM_020983.2	ADCY6	adenylate cyclase 6, transcript variant 2	12	−0.6890	3.5×10^{-4}	0.0464
ILMN_1721087	NM_012435.1	SHC2	SHC (Src homology 2 domain containing) transforming protein 2	19	−0.6788	3.5×10^{-4}	0.0465
ILMN_1700811	NM_019116.2	UBFD1	ubiquitin family domain containing 1	16	0.6888	3.5×10^{-4}	0.0466
ILMN_1661066	XM_927710.1	LOC644596	hypothetical protein LOC644596	X	−0.6663	3.5×10^{-4}	0.0466
ILMN_1733769	NM_001033047.1	NPNT	nephronectin	4	−0.7029	3.5×10^{-4}	0.0466
ILMN_1784948	NM_144569.4	SPOCD1	SPOC domain containing 1	1	−0.7223	3.6×10^{-4}	0.0467
ILMN_1727574	NM_178835.3	LOC152485	hypothetical protein LOC152485		−0.6904	3.5×10^{-4}	0.0467
ILMN_1724984	NM_004836.4	EIF2AK3	eukaryotic translation initiation factor 2-alpha kinase 3	2	0.6981	3.7×10^{-4}	0.0467
ILMN_1660305	NM_177966.4	2′-PDE	2′-phosphodiesterase	3	0.7031	3.5×10^{-4}	0.0468
ILMN_1782057	NM_020452.2	ATP8B2	ATPase, Class I, type 8B, member 2, transcript variant 1	1	−0.7041	3.6×10^{-4}	0.0468
ILMN_1751072	NM_021203.2	SRPRB	signal recognition particle receptor, B subunit	3	0.6672	3.7×10^{-4}	0.0468
ILMN_1740609	NM_032964.2	CCL15	chemokine (C-C motif) ligand 15, transcript variant 1	17	−0.6697	3.7×10^{-4}	0.0468
ILMN_1669982	NM_001080433.1	CCDC85A	coiled-coil domain containing 85A	2	−0.6858	3.6×10^{-4}	0.0468
ILMN_1807515	NM_015235.2	CSTF2T	cleavage stimulation factor, 3′ pre-RNA, subunit 2, 64kDa, tau variant	10	0.6892	3.5×10^{-4}	0.0469
ILMN_1657361	NM_175709.2	CBX7	chromobox homolog 7	22	−0.6904	3.8×10^{-4}	0.0469
ILMN_1801043	NM_198252.2	GSN	gelsolin (amyloidosis, Finnish type), transcript variant 2	9	−0.7028	3.7×10^{-4}	0.0469
ILMN_1738116	NM_181724.1	TMEM119	transmembrane protein 119	12	−0.6425	3.7×10^{-4}	0.0470
ILMN_1760890	NM_206926.1	SEPN1	selenoprotein N, 1, transcript variant 2	1	−0.6762	3.8×10^{-4}	0.0473
ILMN_1728785	NM_015234.4	GPR116	G protein-coupled receptor 116, transcript variant 1	6	−0.6903	3.8×10^{-4}	0.0475
ILMN_1744647	NM_018448.2	CAND1	cullin-associated and neddylation-dissociated 1	12	0.6883	3.9×10^{-4}	0.0479
ILMN_1757440	XM_001130258.1	FAM69B	family with sequence similarity 69, member B	9	−0.6706	3.9×10^{-4}	0.0480
ILMN_1783805	NM_013364.4	PNMA3	paraneoplastic antigen MA3	X	−0.7005	3.9×10^{-4}	0.0482
ILMN_1809098	NM_019599.2	TAS2R1	taste receptor, type 2, member 1	5	0.7013	4.1×10^{-4}	0.0490
ILMN_1719759	NM_002160.2	TNC	tenascin C (hexabrachion)	9	−0.7107	4.1×10^{-4}	0.0491
ILMN_1811313	NM_003062.1	SLIT3	slit homolog 3 (Drosophila)	5	−0.6810	4.0×10^{-4}	0.0491
ILMN_1700432	NM_002221.2	ITPKB	inositol 1,4,5-trisphosphate 3-kinase B	1	−0.6983	4.1×10^{-4}	0.0495
ILMN_1809488	NM_014752.1	SPCS2	signal peptidase complex subunit 2 homolog (S cerevisiae)	11	0.6204	4.2×10^{-4}	0.0498
ILMN_1795338	NM_013313.3	YPEL1	yippee-like 1 (Drosophila)	22	−0.6528	4.3×10^{-4}	0.0505
ILMN_1736242	NM_015432.2	PLEKHG4	pleckstrin homology domain containing, family G (with RhoGef domain) member 4	16	−0.6879	4.3×10^{-4}	0.0506

Illumina ID	GenBank ID	Symbol	Definition	Ch	[b] Beta value	[c] *P* value	[d] FDR *P* value
ILMN_1696568	NM_014382.2	ATP2C1	ATPase, Ca++ transporting, type 2C, member 1, transcript variant 1	3	0.6572	4.3×10^{-4}	0.0507
ILMN_1766925	NM_001257.3	CDH13	cadherin 13, H-cadherin (heart)	16	−0.7020	4.3×10^{-4}	0.0509
ILMN_1698252	NM_152633.2	FANCB	Fanconi anemia, complementation group B, transcript variant 2	X	0.6928	4.5×10^{-4}	0.0526
ILMN_1781149	NM_006774.4	INMT	indolethylamine N-methyltransferase	7	−0.6688	4.6×10^{-4}	0.0530
ILMN_1665437	NM_000773.3	CYP2E1	cytochrome P450, family 2, subfamily E, polypeptide 1	10	−0.6839	4.6×10^{-4}	0.0531
ILMN_1773395	NM_002905.2	RDH5	retinol dehydrogenase 5 (11-cis/9-cis)	12	−0.6860	4.6×10^{-4}	0.0533
ILMN_1665483	NM_014878.4	KIAA0020	KIAA0020	9	0.6892	4.6×10^{-4}	0.0534
ILMN_1666545	NM_001097635.1	GCNT1	glucosaminyl (N-acetyl) transferase 1, core 2 (beta-1,6-N-acetylglucosaminyltransferase), transcript variant 4	9	0.6953	4.6×10^{-4}	0.0535
ILMN_1743864	NM_001453.2	FOXC1	forkhead box C1	6	−0.6694	4.8×10^{-4}	0.0542
ILMN_1709486	NM_006307.3	SRPX	sushi-repeat-containing protein, X-linked	X	−0.6834	4.8×10^{-4}	0.0543
ILMN_1676088	NM_198080.2	MSRB3	methionine sulfoxide reductase B3, transcript variant 1	12	−0.6889	4.8×10^{-4}	0.0543
ILMN_1771238	NM_000390.2	CHM	choroideremia (Rab escort protein 1), transcript variant 1	X	0.6744	4.9×10^{-4}	0.0544
ILMN_1656807	NM_000988.3	RPL27	ribosomal protein L27	17	−0.6987	4.9×10^{-4}	0.0545
ILMN_1711826	NM_020344.1	SLC24A2	solute carrier family 24 (sodium/potassium/calcium exchanger), member 2	9	−0.6804	5.0×10^{-4}	0.0545
ILMN_1660730	NM_032803.4	SLC7A3	solute carrier family 7 (cationic amino acid transporter, y+ system), member 3, transcript variant 1	X	−0.6816	4.9×10^{-4}	0.0546
ILMN_1849218	BX451947	Hs.559564	BX451947 FETAL BRAIN cDNA clone CS0DF008YL16 5-PRIME sequence		−0.6910	4.9×10^{-4}	0.0547
ILMN_1726752	NM_175071.1	APTX	aprataxin, transcript variant 5	9	0.6732	4.9×10^{-4}	0.0548
ILMN_1739640	NM_003737.2	DCHS1	dachsous 1 (Drosophila)	11	−0.6808	5.0×10^{-4}	0.0550
ILMN_1686968	NM_152493.2	FLJ25476	FLJ25476 protein	1	−0.6856	5.1×10^{-4}	0.0557
ILMN_1718044	NM_018127.5	ELAC2	elaC homolog 2 (E coli)	17	−0.6695	5.3×10^{-4}	0.0562
ILMN_1799836	NM_006735.3	HOXA2	homeobox A2	7	−0.7036	5.3×10^{-4}	0.0563
ILMN_1658847	XM_939432.1	MGC61598	similar to ankyrin-repeat protein Nrarp	9	−0.6363	5.3×10^{-4}	0.0565
ILMN_1764619	NM_207443.1	FLJ45244	FLJ45244 protein	14	−0.6691	5.3×10^{-4}	0.0567
ILMN_1739521	NM_014932.2	NLGN1	neuroligin 1	3	0.6893	5.4×10^{-4}	0.0568
ILMN_1710675	NM_005080.2	XBP1	X-box binding protein 1, transcript variant 1	22	0.6814	5.3×10^{-4}	0.0568
ILMN_1772810	XM_946142.2	SHANK3	SH3 and multiple ankyrin repeat domains 3, transcript variant 4	22	−0.6733	5.4×10^{-4}	0.0570
ILMN_1693481	NM_021949.2	ATP2B3	ATPase, Ca++ transporting, plasma membrane 3, transcript variant 1	X	0.6669	5.3×10^{-4}	0.0570
ILMN_1671106	NM_002060.2	GJA4	gap junction protein, alpha 4, 37kDa	1	−0.6706	5.3×10^{-4}	0.0572

Illumina ID	GenBank ID	Symbol	Definition	Ch	[b] Beta value	[c] *P* value	[d] FDR *P* value
ILMN_1773757	NM_138718.1	SLC26A8	solute carrier family 26, member 8, transcript variant 2	6	0.6936	5.5×10^{-4}	0.0573
ILMN_1680652	NM_003944.2	SELENBP1	selenium binding protein 1	1	−0.6566	5.6×10^{-4}	0.0585
ILMN_1813528	NM_133459.1	CCBE1	collagen and calcium binding EGF domains 1	18	−0.6806	5.7×10^{-4}	0.0587
ILMN_1715175	NM_000245.2	MET	met proto-oncogene (hepatocyte growth factor receptor)	7	0.6834	5.7×10^{-4}	0.0587
ILMN_1688160	NM_182552.3	WDR27	WD repeat domain 27	6	−0.6906	5.7×10^{-4}	0.0587
ILMN_1805842	NM_001449.3	FHL1	four and a half LIM domains 1	X	−0.6833	5.6×10^{-4}	0.0587
ILMN_1806301	NM_002077.2	GOLGA1	golgi autoantigen, golgin subfamily a, 1	9	−0.6603	5.8×10^{-4}	0.0595
ILMN_1734653	NM_032532.2	FNDC1	fibronectin type III domain containing 1	6	−0.6810	5.9×10^{-4}	0.0596
ILMN_1706935	NM_022742.3	CCDC136	coiled-coil domain containing 136	7	−0.6766	5.9×10^{-4}	0.0597
ILMN_1727091	NM_138326.2	ACMSD	aminocarboxymuconate semialdehyde decarboxylase	2	0.6688	5.9×10^{-4}	0.0597
ILMN_1740385	NM_014956.4	CEP164	centrosomal protein 164kDa	11	−0.6244	5.9×10^{-4}	0.0598
ILMN_1746517	NM_003937.2	KYNU	kynureninase (L-kynurenine hydrolase), transcript variant 1	2	0.6445	6.0×10^{-4}	0.0598
ILMN_1801246	NM_003641.3	IFITM1	interferon induced transmembrane protein 1 (9–27)	11	−0.6716	6.0×10^{-4}	0.0599
ILMN_1756784	NM_014286.2	FREQ	frequenin homolog (Drosophila)	9	−0.6824	6.1×10^{-4}	0.0599
ILMN_1652389	NM_001031733.2	CALML4	calmodulin-like 4, transcript variant 2	15	−0.6783	6.1×10^{-4}	0.0600
ILMN_1794038	NM_030797.2	FAM49A	family with sequence similarity 49, member A	2	0.6333	6.1×10^{-4}	0.0601
ILMN_1758731	NM_000775.2	CYP2J2	cytochrome P450, family 2, subfamily J, polypeptide 2	1	0.6767	6.1×10^{-4}	0.0602
ILMN_1707380	NM_002725.3	PRELP	proline/arginine-rich end leucine-rich repeat protein, transcript variant 1	1	−0.6844	6.1×10^{-4}	0.0603
ILMN_1801226	NM_020812.1	DOCK6	dedicator of cytokinesis 6	19	−0.6576	6.1×10^{-4}	0.0605
ILMN_1766386	XR_017805.1	LOC401433	hypothetical gene supported by AK127717, misc RNA	7	−0.6178	6.2×10^{-4}	0.0607
ILMN_1763657	NM_025212.1	CXXC4	CXXC finger 4	4	−0.6560	6.3×10^{-4}	0.0608
ILMN_1777221	NM_058182.2	C21orf51	chromosome 21 open reading frame 51	21	−0.6266	6.3×10^{-4}	0.0612
ILMN_1712199	NM_024738.1	C12orf49	chromosome 12 open reading frame 49	12	0.6531	6.4×10^{-4}	0.0619
ILMN_1741801	NM_003503.2	CDC7	cell division cycle 7 homolog (S cerevisiae)	1	0.6725	6.6×10^{-4}	0.0631
ILMN_1891067	AK127526	Hs.553187	cDNA FLJ45619 fis, clone BRTHA3027318		0.6413	6.6×10^{-4}	0.0632
ILMN_1663843	NM_004161.3	RAB1A	RAB1A, member RAS oncogene family	2	0.6529	6.7×10^{-4}	0.0632
ILMN_1792571	NM_173728.2	ARHGEF15	Rho guanine nucleotide exchange factor (GEF) 15	17	−0.6508	6.7×10^{-4}	0.0632
ILMN_1790315	NM_001039706.1	FLJ21062	hypothetical protein FLJ21062	7	−0.6657	6.6×10^{-4}	0.0634
ILMN_1733756	NM_080645.2	COL12A1	collagen, type XII, alpha 1, transcript variant short	6	−0.6799	6.8×10^{-4}	0.0638

Illumina ID	GenBank ID	Symbol	Definition	Ch	[b] Beta value	[c] *P* value	[d] FDR *P* value
ILMN_1812701	NM_001099783.1	C4orf33	chromosome 4 open reading frame 33, transcript variant 2	4	0.6666	6.8×10^{-4}	0.0640
ILMN_1782257	NM_022734.2	METT11D1	methyltransferase 11 domain containing 1, transcript variant 2	14	−0.6653	6.9×10^{-4}	0.0643
ILMN_1691112	NM_176787.4	PIGN	phosphatidylinositol glycan anchor biosynthesis, class N, transcript variant 1	18	0.6741	6.9×10^{-4}	0.0646
ILMN_1756086	NM_023015.3	INTS3	integrator complex subunit 3	1	−0.6306	6.9×10^{-4}	0.0648
ILMN_1710303	NM_031421.2	TTC25	tetratricopeptide repeat domain 25	17	−0.6482	7.0×10^{-4}	0.0651
ILMN_1785765	NM_004800.1	TM9SF2	transmembrane 9 superfamily member 2	13	0.6617	7.1×10^{-4}	0.0656
ILMN_1684321	NM_030579.2	CYB5B	cytochrome b5 type B (outer mitochondrial membrane)	16	0.6858	7.1×10^{-4}	0.0658
ILMN_1722244	NM_001018011.1	ZBTB16	zinc finger and BTB domain containing 16, transcript variant 2	11	−0.6734	7.2×10^{-4}	0.0660
ILMN_1787906	NM_014629.2	ARHGEF10	Rho guanine nucleotide exchange factor (GEF) 10	8	−0.6634	7.3×10^{-4}	0.0668
ILMN_1736974	NM_006943.2	SOX12	SRY (sex determining region Y)-box 12	20	−0.6435	7.4×10^{-4}	0.0668
ILMN_1808590	NM_000856.3	GUCY1A3	guanylate cyclase 1, soluble, alpha 3	4	−0.6252	7.3×10^{-4}	0.0669
ILMN_1751559	NM_024600.2	C16orf30	chromosome 16 open reading frame 30	16	−0.6442	7.4×10^{-4}	0.0671
ILMN_1774427	NM_020898.1	CALCOCO 1	calcium binding and coiled-coil domain 1	12	−0.6804	7.7×10^{-4}	0.0682
ILMN_1657502	NM_001098515.1	MRGPRF	MAS-related GPR, member F, transcript variant 1	11	−0.6781	7.6×10^{-4}	0.0682
ILMN_1652128	NM_018368.2	LMBRD1	LMBR1 domain containing 1	6	0.6306	7.8×10^{-4}	0.0683
ILMN_1808417	NM_015102.2	NPHP4	nephronophthisis 4	1	−0.6615	7.7×10^{-4}	0.0684
ILMN_1657194	NM_018430.2	TSNAXIP1	translin-associated factor X interacting protein 1	16	−0.6513	7.7×10^{-4}	0.0684
ILMN_1680948	NM_012134.2	LMOD1	leiomodin 1 (smooth muscle)	1	−0.6757	7.7×10^{-4}	0.0684
ILMN_1703471	NM_007348.2	ATF6	activating transcription factor 6	1	0.6569	7.6×10^{-4}	0.0684
ILMN_1728742	NM_032385.3	C5orf4	chromosome 5 open reading frame 4, transcript variant 2	5	−0.6564	7.8×10^{-4}	0.0686
ILMN_1702861	NM_172244.2	SGCD	sarcoglycan, delta (35kDa dystrophin-associated glycoprotein), transcript variant 2	5	−0.6460	7.6×10^{-4}	0.0686
ILMN_1868150	BX537697	Hs.98581	mRNA; cDNA DKFZp686D0853 (from clone DKFZp686D0853)		−0.6645	7.9×10^{-4}	0.0686
ILMN_1694325	NM_002501.2	NFIX	nuclear factor I/X (CCAAT-binding transcription factor)	19	−0.6525	7.8×10^{-4}	0.0687
ILMN_1748432	XM_375646.3	ZNF525	zinc finger protein 525	19	0.6710	8.0×10^{-4}	0.0691
ILMN_1743357	NM_003399.5	XPNPEP2	X-prolyl aminopeptidase (aminopeptidase P) 2, membrane-bound	X	−0.6388	8.0×10^{-4}	0.0694
ILMN_1782125	NM_024422.2	DSC2	desmocollin 2, transcript variant Dsc2a	18	0.6142	8.0×10^{-4}	0.0695
ILMN_1687967	NM_001007156.1	NTRK3	neurotrophic tyrosine kinase, receptor, type 3, transcript variant 3	15	−0.6630	8.1×10^{-4}	0.0699
ILMN_1685286	NM_017607.2	PPP1R12C	protein phosphatase 1, regulatory (inhibitor) subunit 12C	19	−0.6754	8.3×10^{-4}	0.0710
ILMN_1756937	NM_005668.3	ST8SIA4	ST8 alpha-N-acetyl-neuraminide alpha-2,8-sialyltransferase 4, transcript variant 1	5	0.6470	8.3×10^{-4}	0.0711

Illumina ID	GenBank ID	Symbol	Definition	Ch	[b] Beta value	[c] *P* value	[d] FDR *P* value
ILMN_1794534	NM_021827.3	CCDC81	coiled-coil domain containing 81	11	−0.6588	8.4×10^{-4}	0.0712
ILMN_1793615	NM_001014811.1	ME3	malic enzyme 3, NADP(+)-dependent, mitochondrial, nuclear gene encoding mitochondrial protein, transcript variant 2	11	−0.6720	8.5×10^{-4}	0.0716
ILMN_1885397	BM311228	Hs.503590	ig62e09y1 HR85 islet cDNA 5 sequence		−0.6606	8.5×10^{-4}	0.0717
ILMN_1759375	NM_001083330.1	ZNF133	zinc finger protein 133, transcript variant 2	20	−0.6532	8.5×10^{-4}	0.0719
ILMN_1796851	XM_001131060.1	FOXL2	forkhead box L2	3	−0.6417	8.6×10^{-4}	0.0720
ILMN_1703105	NM_139178.2	ALKBH3	alkB, alkylation repair homolog 3 (E coli)	11	−0.6275	8.5×10^{-4}	0.0720
ILMN_1678710	NM_032439.1	PHYHIPL	phytanoyl-CoA 2-hydroxylase interacting protein-like	10	0.6064	8.8×10^{-4}	0.0733
ILMN_1758398	NM_000858.4	GUK1	guanylate kinase 1	1	−0.6158	8.9×10^{-4}	0.0735
ILMN_1796734	NM_003118.2	SPARC	secreted protein, acidic, cysteine-rich (osteonectin)	5	−0.6468	8.8×10^{-4}	0.0737
ILMN_1653856	NM_032873.3	STS-1	Cbl-interacting protein Sts-1	11	0.6288	8.9×10^{-4}	0.0739
ILMN_1795251	NM_004684.3	SPARCL1	SPARC-like 1 (mast9, hevin)	4	−0.6301	9.0×10^{-4}	0.0746
ILMN_1717206	NM_175060.1	CLEC14A	C-type lectin domain family 14, member A	14	−0.6376	9.2×10^{-4}	0.0754
ILMN_1739496	NM_006902.3	PRRX1	paired related homeobox 1, transcript variant pmx-1a	1	−0.6477	9.2×10^{-4}	0.0754
ILMN_1718552	NM_006419.1	CXCL13	chemokine (C-X-C motif) ligand 13 (B-cell chemoattractant)	4	−0.6037	9.2×10^{-4}	0.0755
ILMN_1797191	NM_014656.1	KIAA0040	KIAA0040	1	0.6227	9.2×10^{-4}	0.0757
ILMN_1737705	NM_015054.1	KIAA0701	KIAA0701 protein, transcript variant 1	12	0.6459	9.5×10^{-4}	0.0770
ILMN_1682781	NM_003598.1	TEAD2	TEA domain family member 2	19	−0.6440	9.5×10^{-4}	0.0771
ILMN_1673352	NM_006435.2	IFITM2	interferon induced transmembrane protein 2 (1-8D)	11	−0.6409	9.6×10^{-4}	0.0772
ILMN_1750158	NM_007292.4	ACOX1	acyl-Coenzyme A oxidase 1, palmitoyl, transcript variant 2	17	0.6554	9.7×10^{-4}	0.0772
ILMN_1657156	NM_207306.2	KIAA0495	KIAA0495	1	−0.6716	9.7×10^{-4}	0.0773
ILMN_1787576	NM_004070.3	CLCNKA	chloride channel Ka, transcript variant 1	1	−0.6609	9.6×10^{-4}	0.0773
ILMN_1665449	NM_019055.4	ROBO4	roundabout homolog 4, magic roundabout (Drosophila)	11	−0.6256	9.7×10^{-4}	0.0773
ILMN_1796018	NM_004554.3	NFATC4	nuclear factor of activated T-cells, cytoplasmic, calcineurin-dependent 4	14	−0.6726	9.6×10^{-4}	0.0774
ILMN_1765118	NM_003627.4	SLC43A1	solute carrier family 43, member 1	11	−0.6174	9.9×10^{-4}	0.0784
ILMN_1785424	NM_006720.3	ABLIM1	actin binding LIM protein 1, transcript variant 4	10	−0.6004	9.9×10^{-4}	0.0784
ILMN_1701204	NM_005429.2	VEGFC	vascular endothelial growth factor C	4	−0.6393	9.9×10^{-4}	0.0784
ILMN_1769186	NM_001755.2	CBFB	core-binding factor, beta subunit, transcript variant 2	16	0.6454	1.0×10^{-3}	0.0785
ILMN_1651958	NM_000900.2	MGP	matrix Gla protein	12	−0.6404	1.0×10^{-3}	0.0786

Illumina ID	GenBank ID	Symbol	Definition	Ch	[b] Beta value	[c] *P* value	[d] FDR *P* value
ILMN_1770803	NM_004330.1	BNIP2	BCL2/adenovirus E1B 19kDa interacting protein 2	15	0.6074	1.0×10^{-3}	0.0786
ILMN_1720452	NM_001031855.1	LONRF3	LON peptidase N-terminal domain and ring finger 3, transcript variant 1	X	0.6477	1.0×10^{-3}	0.0786
ILMN_1780349	NM_003292.2	TPR	translocated promoter region (to activated MET oncogene)	1	−0.6328	1.0×10^{-3}	0.0792
ILMN_1818018	DA321576	Hs.576997	DA321576 BRHIP3 cDNA clone BRHIP3014850 5 sequence		0.6451	1.0×10^{-3}	0.0793
ILMN_1724424	NM_145239.1	PRRT2	proline-rich transmembrane protein 2	16	−0.6496	1.0×10^{-3}	0.0794
ILMN_1760849	NM_018092.3	NETO2	neuropilin (NRP) and tolloid (TLL)-like 2	16	0.6201	1.0×10^{-3}	0.0794
ILMN_1773742	NM_012328.1	DNAJB9	DnaJ (Hsp40) homolog, subfamily B, member 9	7	0.6452	1.0×10^{-3}	0.0794
ILMN_1792529	NM_004783.2	TAOK2	TAO kinase 2, transcript variant 1	16	−0.6358	1.0×10^{-3}	0.0796
ILMN_1740772	NM_133172.2	APBB3	amyloid beta (A4) precursor protein-binding, family B, member 3, transcript variant 3	5	−0.6393	1.1×10^{-3}	0.0796
ILMN_1737604	NM_018291.2	FLJ10986	hypothetical protein FLJ10986	1	0.6581	1.0×10^{-3}	0.0796
ILMN_1742272	NM_000537.2	REN	renin	1	−0.6262	1.1×10^{-3}	0.0798
ILMN_1806403	NM_016563.2	RASL12	RAS-like, family 12	15	−0.6338	1.1×10^{-3}	0.0798
ILMN_1715647	NM_020335.1	VANGL2	vang-like 2 (van gogh, Drosophila)	1	−0.6544	1.1×10^{-3}	0.0800
ILMN_1655913	NM_005013.2	NUCB2	nucleobindin 2	11	0.6408	1.1×10^{-3}	0.0801
ILMN_1736080	NM_012432.2	SETDB1	SET domain, bifurcated 1	1	−0.6417	1.1×10^{-3}	0.0805
ILMN_1663033	NM_138385.2	TMEM129	transmembrane protein 129	4	−0.6319	1.1×10^{-3}	0.0809
ILMN_1697585	NM_022496.3	ACTR6	ARP6 actin-related protein 6 homolog (yeast)	12	0.6055	1.1×10^{-3}	0.0817
ILMN_1711124	NM_144724.1	MARVELD2	MARVEL domain containing 2, transcript variant 2	5	0.6463	1.1×10^{-3}	0.0820
ILMN_1711919	NM_017988.4	SCYL2	SCY1-like 2 (S cerevisiae)	12	0.5937	1.1×10^{-3}	0.0821
ILMN_1669142	NM_057175.3	NARG1	NMDA receptor regulated 1	4	0.6007	1.1×10^{-3}	0.0822
ILMN_1678862	NM_173540.2	FUT11	fucosyltransferase 11 (alpha (1,3) fucosyltransferase)	10	0.6192	1.1×10^{-3}	0.0822
ILMN_1768393	NM_006938.2	SNRPD1	small nuclear ribonucleoprotein D1 polypeptide 16kDa	18	0.5974	1.1×10^{-3}	0.0822
ILMN_1782938	NM_018593.3	SLC16A10	solute carrier family 16, member 10 (aromatic amino acid transporter)	6	0.5965	1.1×10^{-3}	0.0822
ILMN_1899428	AW173494	Hs.483540	xj07f12x1 NCI_CGAP_Ut2 cDNA clone IMAGE:2656559 3 sequence		−0.6320	1.1×10^{-3}	0.0825
ILMN_1748845	NM_002506.2	NGFB	nerve growth factor, beta polypeptide	1	−0.6390	1.1×10^{-3}	0.0832
ILMN_1767722	NM_203437.2	AFTPH	aftiphilin, transcript variant 1	2	0.6445	1.2×10^{-3}	0.0837
ILMN_1791545	NM_015515.3	KRT23	keratin 23 (histone deacetylase inducible)	17	0.6391	1.2×10^{-3}	0.0838
ILMN_1747183	NM_001099650.1	GLT8D3	glycosyltransferase 8 domain containing 3, transcript variant 2	12	0.6353	1.2×10^{-3}	0.0839
ILMN_1815666	NM_170665.2	ATP2A2	ATPase, Ca++ transporting, cardiac muscle, slow twitch 2, transcript variant 1	12	0.6340	1.2×10^{-3}	0.0840

Illumina ID	GenBank ID	Symbol	Definition	Ch	[b] Beta value	[c] *P* value	[d] FDR *P* value
ILMN_1761425	NM_182487.2	OLFML2A	olfactomedin-like 2A	9	−0.6347	1.2×10^{-3}	0.0843
ILMN_1794825	NM_000382.2	ALDH3A2	aldehyde dehydrogenase 3 family, member A2, transcript variant 2	17	−0.6101	1.2×10^{-3}	0.0845
ILMN_1767459	NM_018082.4	POLR3B	polymerase (RNA) III (DNA directed) polypeptide B	12	0.6220	1.2×10^{-3}	0.0851
ILMN_1717905	NM_015726.2	WDR42A	WD repeat domain 42A	1	−0.6202	1.2×10^{-3}	0.0853
ILMN_1682404	NM_006515.1	SETMAR	SET domain and mariner transposase fusion gene	3	−0.6306	1.2×10^{-3}	0.0861
ILMN_1725338	NM_194284.2	CLDN23	claudin 23	8	0.6369	1.2×10^{-3}	0.0863
ILMN_1765371	NM_018032.3	LUC7L	LUC7-like (S cerevisiae), transcript variant 1	16	−0.6428	1.2×10^{-3}	0.0863
ILMN_1756118	NM_014634.2	PPM1F	protein phosphatase 1F (PP2C domain containing)	22	−0.5914	1.2×10^{-3}	0.0864
ILMN_1793621	NM_001002262.1	ZFYVE27	zinc finger, FYVE domain containing 27, transcript variant 3	10	0.6345	1.2×10^{-3}	0.0865
ILMN_1654945	NM_153759.2	DNMT3A	DNA (cytosine-5-)-methyltransferase 3 alpha, transcript variant 2	2	0.6434	1.2×10^{-3}	0.0866
ILMN_1754364	NM_001868.1	CPA1	carboxypeptidase A1 (pancreatic)	7	0.6196	1.2×10^{-3}	0.0866
ILMN_1663640	NM_000240.2	MAOA	monoamine oxidase A, nuclear gene encoding mitochondrial protein	X	0.6353	1.3×10^{-3}	0.0874
ILMN_1728581	NM_016210.2	C3orf18	chromosome 3 open reading frame 18	3	−0.6159	1.3×10^{-3}	0.0876
ILMN_1736834	NM_005414.2	SKIL	SKI-like oncogene	3	0.6206	1.3×10^{-3}	0.0883
ILMN_1800731	NM_018328.3	MBD5	methyl-CpG binding domain protein 5	2	−0.6235	1.3×10^{-3}	0.0884
ILMN_1805098	NM_000924.2	PDE1B	phosphodiesterase 1B, calmodulin-dependent	12	−0.6434	1.3×10^{-3}	0.0884
ILMN_1769764	NM_001039935.1	ANKRD55	ankyrin repeat domain 55, transcript variant 2	5	0.6090	1.3×10^{-3}	0.0885
ILMN_1814015	NM_004063.2	CDH17	cadherin 17, LI cadherin (liver-intestine)	8	−0.6315	1.3×10^{-3}	0.0885
ILMN_1802669	NM_021132.1	PPP3CB	protein phosphatase 3 (formerly 2B), catalytic subunit, beta isoform	10	−0.6361	1.3×10^{-3}	0.0888
ILMN_1800512	NM_002133.1	HMOX1	heme oxygenase (decycling) 1	22	0.5922	1.3×10^{-3}	0.0888
ILMN_1772731	NM_005326.4	HAGH	hydroxyacylglutathione hydrolase, transcript variant 1	16	−0.6280	1.3×10^{-3}	0.0890
ILMN_1756573	NM_020142.3	NDUFA4L2	NADH dehydrogenase (ubiquinone) 1 alpha subcomplex, 4-like 2	12	−0.6186	1.3×10^{-3}	0.0891
ILMN_1686464	NM_180991.4	SLCO4C1	solute carrier organic anion transporter family, member 4C1	5	0.6381	1.3×10^{-3}	0.0903
ILMN_1769083	NM_000847.3	GSTA3	glutathione S-transferase A3	6	0.6117	1.3×10^{-3}	0.0904
ILMN_1687410	NM_022776.3	OSBPL11	oxysterol binding protein-like 11	3	0.6035	1.4×10^{-3}	0.0918
ILMN_1651611	NM_000527.2	LDLR	low density lipoprotein receptor (familial hypercholesterolemia)	19	0.6122	1.4×10^{-3}	0.0937
ILMN_1665123	NM_178177.2	NMNAT3	nicotinamide nucleotide adenylyltransferase 3	3	−0.6152	1.4×10^{-3}	0.0938
ILMN_1651370	NM_001014443.2	USP21	ubiquitin specific peptidase 21, transcript variant 3	1	−0.6228	1.4×10^{-3}	0.0939
ILMN_1774110	NM_004067.2	CHN2	chimerin (chimaerin) 2, transcript variant 2	7	0.6275	1.4×10^{-3}	0.0950

Illumina ID	GenBank ID	Symbol	Definition	Ch	[b] Beta value	[c] *P* value	[d] FDR *P* value
ILMN_1730662	NM_001008745.1	LOC401431	hypothetical gene LOC401431	7	−0.6048	1.4×10^{-3}	0.0950
ILMN_1753554	NM_022763.2	FNDC3B	fibronectin type III domain containing 3B	3	0.6167	1.4×10^{-3}	0.0950
ILMN_1734254	NM_014106.2	ZNF770	zinc finger protein 770	15	0.5801	1.4×10^{-3}	0.0951
ILMN_1801889	NM_015011.1	MYO16	myosin XVI	13	−0.6401	1.4×10^{-3}	0.0951
ILMN_1703074	NM_001304.3	CPD	carboxypeptidase D	17	0.6178	1.4×10^{-3}	0.0952
ILMN_1885728	XM_001130020.1	KIAA1147	KIAA1147	7	0.6203	1.5×10^{-3}	0.0952
ILMN_1652594	NM_024855.3	ACTR5	ARP5 actin-related protein 5 homolog (yeast)	20	−0.6197	1.4×10^{-3}	0.0953
ILMN_1672287	NM_018657.3	MYNN	myoneurin	3	0.6237	1.5×10^{-3}	0.0954
ILMN_1680113	NM_004758.1	BZRAP1	benzodiazapine receptor (peripheral) associated protein 1	17	−0.6340	1.5×10^{-3}	0.0966
ILMN_1660282	NM_022135.2	POPDC2	popeye domain containing 2	3	−0.6316	1.5×10^{-3}	0.0967
ILMN_1683441	NM_015261.2	NCAPD3	non-SMC condensin II complex, subunit D3	11	−0.6169	1.5×10^{-3}	0.0968
ILMN_1761486	NM_024808.2	C13orf34	chromosome 13 open reading frame 34	13	0.6187	1.5×10^{-3}	0.0970
ILMN_1894569	BX093121	Hs.571048	BX093121 Soares_placenta_8to9weeks_2NbHP8to9W cDNA clone IMAGp998K13561; IMAGE:257796 sequence		0.6106	1.5×10^{-3}	0.0970
ILMN_1751086	NM_015459.3	DKFZP564J086D	DKFZP564J0863 protein	11	0.5780	1.5×10^{-3}	0.0970
ILMN_1656386	NM_014822.1	SEC24D	SEC24 related gene family, member D (S cerevisiae)	4	0.6073	1.5×10^{-3}	0.0971
ILMN_1760271	NM_194314.2	ZBTB41	zinc finger and BTB domain containing 41	1	0.6038	1.5×10^{-3}	0.0972
ILMN_1702683	NM_004733.2	SLC33A1	solute carrier family 33 (acetyl-CoA transporter), member 1	3	0.6196	1.5×10^{-3}	0.0972
ILMN_1878019	AL512695	Hs.278285	mRNA; cDNA DKFZp547G133 (from clone DKFZp547G133)		0.6348	1.5×10^{-3}	0.0973
ILMN_1806487	NM_001002034.2	FAM109B	family with sequence similarity 109, member B	22	−0.5735	1.5×10^{-3}	0.0973
ILMN_1779748	NM_004192.2	ASMTL	acetylserotonin O-methyltransferase-like	X, Y	−0.6146	1.5×10^{-3}	0.0974
ILMN_1770084	NM_006283.1	TACC1	transforming, acidic coiled-coil containing protein 1	8	−0.6145	1.6×10^{-3}	0.0974
ILMN_1707534	NM_017544.2	NKRF	NF-kappaB repressing factor	X	0.6044	1.6×10^{-3}	0.0974
ILMN_1678086	NM_138770.1	CCDC74A	coiled-coil domain containing 74A	2	−0.6070	1.6×10^{-3}	0.0975
ILMN_1669064	NM_001080493.2	HSZFP36	ZFP-36 for a zinc finger protein	19	0.6087	1.5×10^{-3}	0.0975
ILMN_1810093	NM_005725.3	TSPAN2	tetraspanin 2	1	−0.5941	1.5×10^{-3}	0.0976
ILMN_1673522	NM_017947.1	MOCOS	molybdenum cofactor sulfurase	18	0.6122	1.6×10^{-3}	0.0976
ILMN_1764309	NM_000667.2	ADH1A	alcohol dehydrogenase 1A (class I), alpha polypeptide	4	−0.6229	1.6×10^{-3}	0.0977
ILMN_1795325	NM_001615.3	ACTG2	actin, gamma 2, smooth muscle, enteric	2	−0.6151	1.6×10^{-3}	0.0977

Illumina ID	GenBank ID	Symbol	Definition	Ch	[b] Beta value	[c] *P* value	[d] FDR *P* value
ILMN_1773814	NM_205853.2	MUSTN1	musculoskeletal, embryonic nuclear protein 1	3	−0.6206	1.5×10^{-3}	0.0977
ILMN_1703576	NM_012334.2	MYO10	myosin X	5	0.6086	1.6×10^{-3}	0.0977
ILMN_1780937	NM_025128.3	MUS81	MUS81 endonuclease homolog (S cerevisiae)	11	−0.6341	1.6×10^{-3}	0.0977
ILMN_1757162	XM_945736.2	LOC654085	similar to Glycine cleavage system H protein, mitochondrial precursor, transcript variant 2	19	0.6181	1.5×10^{-3}	0.0977
ILMN_1832155	AK094744	Hs.167721	cDNA FLJ37425 fis, clone BRAWH2001530		−0.6007	1.6×10^{-3}	0.0977
ILMN_1782688	NM_024838.4	THNSL1	threonine synthase-like 1 (S cerevisiae)	10	0.6374	1.6×10^{-3}	0.0977
ILMN_1757298	NM_018167.3	BTBD7	BTB (POZ) domain containing 7, transcript variant 2	14	0.6056	1.6×10^{-3}	0.0978
ILMN_1798975	NM_005228.3	EGFR	epidermal growth factor receptor (erythroblastic leukemia viral (v-erb-b) oncogene homolog, avian), transcript variant 1	7	0.6186	1.6×10^{-3}	0.0978
ILMN_1775974	NM_019012.2	PLEKHA5	pleckstrin homology domain containing, family A member 5	12	0.5995	1.6×10^{-3}	0.0979
ILMN_1872404	AK055652	Hs.478682	cDNA FLJ31090 fis, clone IMR321000102		−0.6351	1.6×10^{-3}	0.0979
ILMN_1808999	NM_153213.3	ARHGEF19	Rho guanine nucleotide exchange factor (GEF) 19	1	−0.6104	1.6×10^{-3}	0.0979
ILMN_1733703	NM_018006.4	TRMU	tRNA 5-methylaminomethyl-2-thiouridylate methyltransferase, nuclear gene encoding mitochondrial protein, transcript variant 1	22	−0.6098	1.6×10^{-3}	0.0980
ILMN_1795574	XM_928045.1	LOC644968	hypothetical protein LOC644968	4	0.5916	1.6×10^{-3}	0.0980
ILMN_1700994	NM_001039571.1	KREMEN1	kringle containing transmembrane protein 1, transcript variant 4	22	0.6255	1.6×10^{-3}	0.0980
ILMN_1737146	NM_014294.4	TRAM1	translocation associated membrane protein 1	8	0.6212	1.6×10^{-3}	0.0980
ILMN_1809889	NM_173510.1	CCDC117	coiled-coil domain containing 117	22	0.6109	1.6×10^{-3}	0.0981
ILMN_1735909	NM_001033678.2	TRPT1	tRNA phosphotransferase 1, transcript variant 1	11	−0.6155	1.6×10^{-3}	0.0982
ILMN_1670472	NM_014613.2	UBXD8	UBX domain containing 8	5	0.6387	1.7×10^{-3}	0.0986
ILMN_1700633	NM_022060.2	ABHD4	abhydrolase domain containing 4	14	−0.5964	1.7×10^{-3}	0.0988
ILMN_1914072	BQ718005	Hs.562762	AGENCOURT_8100698 Lupski_sympathetic_trunk cDNA clone IMAGE:6190431 5 sequence		0.6098	1.7×10^{-3}	0.0989
ILMN_1651642	NM_152742.1	GPC2	glypican 2	7	−0.6187	1.7×10^{-3}	0.0990
ILMN_1671046	NM_001541.2	HSPB2	heat shock 27kDa protein 2	11	−0.6162	1.7×10^{-3}	0.0990
ILMN_1662578	NM_020156.1	C1GALT1	core 1 synthase, glycoprotein-N-acetylgalactosamine 3-beta-galactosyltransferase, 1	7	0.5897	1.7×10^{-3}	0.0990
ILMN_1693514	NM_001014795.1	ILK	integrin-linked kinase, transcript variant 3	11	−0.6264	1.7×10^{-3}	0.0992
ILMN_1800447	NM_001031835.1	PHKB	phosphorylase kinase, beta, transcript variant 2	16	0.5895	1.7×10^{-3}	0.0992
ILMN_1701933	NM_007308.1	SNCA	synuclein, alpha (non A4 component of amyloid precursor), transcript variant NACP112	4	−0.5903	1.7×10^{-3}	0.0993
ILMN_1779547	NM_006665.2	HPSE	heparanase	4	0.6297	1.7×10^{-3}	0.0995
ILMN_1883624	DA589983	Hs.582952	DA589983 HLUNG2 cDNA clone HLUNG2011800 5 sequence		0.5802	1.7×10^{-3}	0.0997

Illumina ID	GenBank ID	Symbol	Definition	Ch	[b] Beta value	[c] *P* value	[d] FDR *P* value
ILMN_1774717	NM_020182.3	TMEPAI	transmembrane, prostate androgen induced RNA, transcript variant 1	20	−0.5933	1.7×10^{-3}	0.0998
ILMN_1789463	NM_021902.2	FXYD1	FXYD domain containing ion transport regulator 1 (phospholemman), transcript variant b	19	−0.6164	1.7×10^{-3}	0.0999
ILMN_1651900	NM_002233.2	KCNA4	potassium voltage-gated channel, shaker-related subfamily, member 4	11	0.6164	1.7×10^{-3}	0.0999

[a] Gene expression in decidual tissue from preeclamptic and normal pregnancies has been compared.

[b] Values are given in beta, a measure of distance between the group means, expressed in SD units. A positive beta implies an up-regulation and a negative beta implies a down-regulation in the preeclamptic group compared to the normal pregnant group.

[c] $P < 0.05$, obtained with SOLAR.

[d] False discovery rate $P < 0.10$.

TABLE 3

Results for the selected genes from microarray and RT-qPCR expression

		Microarray		RT-qPCR	
Gene symbol	**Up/down**	**Beta value**	**[a] *P* value**	**Fold change**	**[b] *P* value**
SLITRK4	↓	−1.04	4.59×10^{-8}	−1.98	<0.0001
FZD4	↓	−0.91	4.05×10^{-7}	−1.35	0.001
ANGPTL2	↓	−0.89	4.39×10^{-6}	−1.74	<0.0001
PLA2G7	↑	0.83	1.58×10^{-5}	1.26	0.068
MAN1A	↑	0.85	1.29×10^{-5}	1.30	0.025
ARL5B	↑	0.91	4.46×10^{-7}	1.22	0.017

[a] *P* <0.001, obtained with SOLAR.

[b] *P* <0.10, obtained with t-test statistics with SPSS software (version 16; SPSS Inc, Chicago, IL).

TABLE 4

Canonical pathway analysis

[a] Canonical Pathway	Genes	[b] *P* value Ingenuity Pathway Analysis	[c] *P* value Rotation Gene Set Enrichment Analysis
Tryptophan metabolism	ACMSD, ALDH3A2, ASMTL, CYP2E1, CYP2J2, INMT, KYNU, MAOA	5.51×10^{-4}	2.0×10^{-4}
Endoplasmic retuculum stress pathway	ATF6, DNAJC3, EIF2AK3, XBP1	5.81×10^{-4}	5.3×10^{-3}
Linoleic acid metabolism	CYP2E1, CYP2J2, PLA2G5, PLA2G2A, WISP2	3.91×10^{-3}	1.5×10^{-3}
Notch signalling	DTX3, HES1, NOTCH3, NOTCH4	6.72×10^{-3}	7.9×10^{-3}
Fatty acid metabolism	ACOX1, ACOX2, ADH1A, ALDH3A2, CYP2E1, CYP2J2	7.90×10^{-3}	10.0×10^{-5}
Arachidonic acid metabolism	CYP2E1, CYP2J2, PLA2G5, PLA2G2A, PTGIS, WISP2	8.66×10^{-3}	10.0×10^{-5}
NRF2-mediated oxidative stress Response	ACTG2, DNAJB6, DNAJB9, DNAJB11, DNAJC3, EIF2AK3, GSTA3, HMOX1, UBE2K	9.99×10^{-3}	6.7×10^{-2}

[a] Ingenuity Pathway Analysis (Ingenuity® Systems, www.ingenuity.com) was used to bioinformatically identify canonical (i.e. cell signalling and metabolic) pathways potentially involved in preeclampsia within our data set.

[b] *P* value obtained with Fisher's exact test.

[c] *P* value obtained with use of the *limma* package.